

Experimental analyses of step extent and contact buffer in pedestrian dynamics

Peter Thompson^{a,b,*}, Hossein Taviana^c, Cathy Goulding^d, Håkan Frantzich^a, Karen Boyce^c, Daniel Nilsson^e, Gabriel Larsson^a, Jesper Friholm^a, Denise McGrath^d

^a Division of Fire Safety Engineering, Lund University, John Ericssons väg 1, Box 118, 221 00 Lund, Sweden

^b Autodesk, Inc., 111 McInnis Parkway, San Rafael, CA 94903, USA

^c FireSERT Centre, Belfast School of Architecture and the Built Environment, Ulster University, Belfast BT15 1ED, UK

^d School of Public Health Physiotherapy and Sports Science, University College Dublin, Woodview House Belfield Dublin 4, Ireland

^e Civil and Natural Resources Engineering Department, University of Canterbury, Christchurch 8140, New Zealand

ARTICLE INFO

Article history:

Received 24 September 2021

Received in revised form 22 December 2021

Available online 24 January 2022

Keywords:

Pedestrian dynamics model

Optical motion capture

Detailed video analysis

Step extent

Contact buffer

Inter-person distance (headway)

ABSTRACT

This study aims to quantify and develop a deeper understanding of the parameters that underpin the development of a new, predictive, microscopic model of pedestrian movement with the potential to accurately reflect the complexity of flow dynamics now and into the future. It presents the results and analyses of two single file experiments designed to quantify the physical space taken up by the extent of a person's stepping movement (maximum step extent) and the minimum distance between points of inter-person contact (contact buffer) across a range of walking speeds.

The experiments successfully used high-resolution optical motion capture and enhanced video analysis to quantify the dynamic changes in gait and spatial parameters, which were manifested as overlapping steps, and changes to step extent, step length, step frequency, and contact distance. The sum of the step extent and contact buffer, at different speeds, was found to be within a few centimetres of the inter-person distance (headway), leading to the conclusion that these parameters are therefore key components for the derivation of inter-person spacing and, hence, overall crowd movement. The work informs the longer term aim of developing the mathematical model which has the potential to include pedestrian demographics, walking ability and cognitive capabilities.

© 2022 The Authors. Published by Elsevier B.V. This is an open access article under the CC BY license (<http://creativecommons.org/licenses/by/4.0/>).

1. Introduction

Walking is a primary mode of transportation. It is a critical requirement to design the built environment to cater for the safe evacuation and efficient movement of pedestrians, particularly in our increasingly populated urban settings. The study of pedestrian movement is an interdisciplinary field in which a variety of methodological approaches have been adopted to model pedestrian dynamics in an effort to optimise crowd flow in the real world. These approaches range from the application of “macroscopic” [1] or “mesoscopic” [2] models, where the crowd is characterised by averaged quantities such as density, velocity and flow, producing well-known ‘fundamental’ diagrams—to more “microscopic” models [3], where

* Corresponding author at: Division of Fire Safety Engineering, Lund University, John Ericssons väg 1, Box 118, 221 00 Lund, Sweden.
E-mail address: pete.thompson@brand.lth.se (P. Thompson).

pedestrians are modelled individually, but traditionally still use relatively standard aggregate parameters of movement, established many years ago.

Globally we are an ageing society with virtually every country in the world experiencing growth in the numbers and percentages of older persons [4]. Obesity has also become increasingly common [5]. Increasing numbers of older people, individuals who are obese, and those with mobility and other impairments have the potential to significantly impact flow dynamics [6–8]. Indeed, researchers who formulated the long established and commonly used speed/flow/density relationships (fundamental diagrams) in pedestrian movement [9,10] have recently questioned the suitability of such out-dated relationships to accurately characterise the flow dynamics of diverse building populations of today [11]. It is therefore increasingly important that we develop predictive, microscopic models of movement that are capable of characterising diverse individuals, their movement and interactions with others, i.e., models which can accurately reflect the complexity of flow dynamics now and in the future [12].

Our previous work [8] developed a preliminary “movement adaption” model for crowd flow (summarised below) that breaks down inter-person distance (aka headway) into component biomechanical variables derived from step length and the distance observed between pedestrians, anticipating that these variables may vary according to age and mobility restrictions, among other factors. Implementation of this model on initial benchmark datasets (derived from [7]) has shown that it can produce predictions of different walking speeds and different flow rates as a function of inter-person distance, depending on age and other demographics [8]. However, much more work is needed in order to corroborate and inform future developments. The main objective of this study was therefore to quantify and develop a deeper understanding of the parameters that underpin the model and their interrelationships. In so doing, we explored different measurement approaches to quantify the parameters under investigation.

1.1. Theory: analysing the movement and adaption components of crowd flow

[8] described the initial prototyping work for analysing the step movement and contact adaption to relate to crowd movement analysis. The basic principle of the analysis, illustrated in Fig. 1, is that inter-person distance between people in single file flow may consist of the sum of:

- *maximum step extent*: the maximum physical space taken up by the extent of a person’s step movement action (measured from the rearmost point of a person’s back foot to the foremost point of the front foot), for a given step cycle. Note that, in normal walking, the step extent will never be equal to the sum of the step length plus foot length because the heels are never simultaneously in contact with the floor unless the person is at a standstill.

- *minimum contact distance*: the minimum distance measured between the closest points of potential contact (toe to heel in single file flow), where space may be left to adapt to changes in movement ahead, identified as “contact buffer”.

Therefore, the inter-person distance between two people A and B is expressed as the contact buffer + the mean of the maximum step extents of both people.

The basic equations of movement are defined thus:

$$\text{During the gait cycle: } C_b = \min(C_d) \quad (1)$$

$$S_{e(max)} = A(S_t + f_l) \quad (2)$$

$$\text{For two people with identical gait: } IPD = S_{e(max)} + C_b \quad (3)$$

$$\text{For two different people A, B: } IPD = \mu S_{e(max)} \{PersonA, PersonB\} + C_b \quad (4)$$

$$q = \frac{V}{IPD} \quad (5)$$

where the parameters are:

- C_d = the distance between potential heel/toe contact points, tracked through its variation during the gait cycle, and referred to as the ‘contact distance’
- C_b = the minimum contact distance tracked during a gait cycle, and referred to as the “contact buffer”
- IPD = the inter-person distance between the centroids of people, sometimes measured at the head, shoulder or hip level of people walking
- S_e is the ‘step extent’, measured from the rearmost point of the heel to the foremost point of the toe during the step cycle
- $S_{e(max)}$ is the maximum ‘step extent’ measured during the step cycle, measured from the rearmost point of the heel to the foremost point of the toe, related to step length and foot length
- $\mu S_{e(max)} \{PersonA, PersonB\}$ is the mean ‘max. step extent’ of Person A and Person B
- A = the proportion of the sum of step length and foot length evaluating to maximum ‘step extent’
- S_t is the standard measure of step length, defined as the distance between two successive heel strikes on the ground for a pedestrian, during one gait cycle of a single step.
- f_l = is foot length

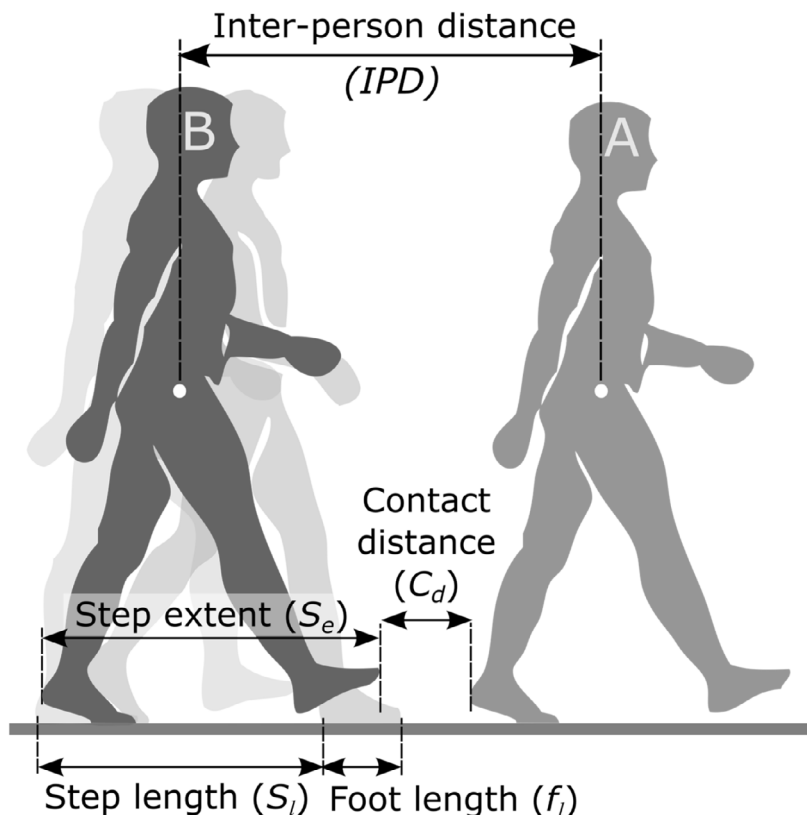


Fig. 1. The step extent and contact distance components in single file crowd flow (showing experimental markers as circles).

- q = flow rate (people/second)
- V = walking speed.

Early explorations [8] of these parameters highlighted the potential value of breaking down individual and inter-person gait into its constituent parts and understanding how these parts may ultimately affect overall flow (Eq. (5)), and be modified for predictive purposes.

Several researchers have already explored some of these microscopic parameters and their interrelationships. For example, the relationship between step length and speed has been studied in situations with and without longitudinal interaction but with variable conclusions. [13] and [14] determined this relationship to be linear when there was no longitudinal interaction, whilst others [15,16] established non-linear relationships. [17] also established a linear relationship between step length and speed when there was longitudinal interaction (for speeds in the range 0.2 and 1.1 m/s and densities 0–1.2 ped/m). [18], however, explored the relationship in situations with and without longitudinal interaction (for densities 0–1.7 ped/m) and concluded that a power function more reliably represented this relationship.

It is also known that individual characteristics such as age [19] and body height [20] may influence step length at given speeds. The influence of height, however, may be reduced when there is longitudinally limited space, which might restrict gait movement. For example, [21] concluded that, in cases without longitudinal interaction (densities ranging from 0.36 to 1.2 ped/m) the step length increased with height; however, when there was longitudinal interaction (densities ranging from 1.2 to 2.35 ped/m), height had no perceivable influence on step length.

The relationship between speed and inter-person distance has also been explored, and is a key reference point for checking parametric relationships. For example, [22] found a linear relationship between speed and inter-person distance for speeds in the range approximately 0.15–1 m/s (densities in the range 0.87–1.96 ped/m). [7] explored the relationship between speed and inter-person distance (headway) for young persons (16–18 years), older adults (45–73 years) and mixed groups in the density range of 0.19 to 2.76 ped/m. They found that the nature of the relationship varied depending on the age of the group. Furthermore, they also established that the point at which speed became independent of headway, i.e., after which pedestrians walked at their preferred speeds (the free regime as defined by [17,23]) varied by group (1.1 m for young group, 1.6 m for the older group and 2.9 m for the mixed group).

Comparison of our prototype model with experimental data [8] suggests that the model is capable of reproducing appropriate trends with regards to speed and flow in single file movement. However, in order to further test and validate

this model, more empirical data and understanding of the inter-relationships between the parameters of movement are required. In particular, it is important to improve our understanding of the relationship between the gait cycle and walking speed in crowded conditions. It is also important to further explore the relationship between inter-person distance and walking speed across a wider range of walking speeds. Of particular importance in confirming the model is the quantification of the contact buffer (a parameter not defined, nor explored in other literature to date) across a range of conditions and speeds and confirmation that the inter-person distance can indeed be considered as a sum of its constituent parts, i.e., step extent plus contact buffer. The primary objective of this study was, therefore, to quantify the parameters (IPD , S_e , C_b , S_l , A) and their interrelationships and the related values of q and v in order to inform, validate, or modify the proposed model.

A number of different experimental designs and data collection methods have been used to explore people/crowd movement. Many studies at the microscopic level have investigated the movement of people walking in single file at different densities which are varied by altering the number of individuals in a fixed path [7,18,21,22,24]). A common approach to data collection has been to use video capture from above, e.g., [18,21], [25] and/or perpendicular to the pathway ([22,24] with the possibility of triangulating to provide 3D measurements. Analysis is then conducted manually (frame by frame) or automatically using image processing software, e.g., Persias [26], PeTrack [7,27].

However, high accuracy measurements of biomechanical characteristics in individuals walking together is a considerable challenge, given the distortions of 2D video analysis, possible tracking errors and occlusions in line-of-sight. Another, albeit less common approach, has been to utilise optical motion capture systems (e.g. Vicon or Qualisys) using passive or active markers and infrared cameras to undertake 3D tracking of each person's head position at high sampling rates [17]. While this may be a more accurate quantification method, it is still vulnerable to line-of-sight issues. The spatial variables being targeted in this study, i.e., step extent, and in particular, contact buffer are on a relatively small scale, so tolerance for error is low.

In this study, two different approaches were used to quantify individual and inter-person variables and their inter-relationships across a range of walking speeds. The first experiment which was conducted at University College Dublin (UCD), Ireland, used high resolution 3D optical motion capture, with an accuracy of approximately ± 0.2 mm, in a single-file laboratory experiment performed with a small number of individuals. In this experiment, researchers had a high degree of control. This enabled an in-depth exploration of changes in contact buffer and step extent across varying, prescribed gait speeds. The conditions in this experiment were akin to a situation in which individuals have a bound velocity due to a slower leader but still have some freedom to choose the distance from their leader. The second experiment, which was conducted at Lund University, Sweden, used enhanced 2D video analysis to inspect a single file experiment. In these trials the number of participants varied, and the speeds of individuals were not controlled but rather were an artifact of the numbers and hence densities in the route. The same variables were measured in two different experimental conditions, with two different approaches in order to investigate the feasibility of capturing these variables using the more widely available 2D video analysis set-up.

2. Methods

2.1. Experiment A (UCD)

Experiment A describes the work carried out on UCD premises, using optical motion capture techniques to measure markers at different points on the bodies of the participants.

Participants:

Sixteen participants (aged 25–48 yrs) were recruited via a recruitment poster at the University College Dublin, Ireland. Participants were not reimbursed for taking part, and also were excluded if they were carrying any acute lower limb injuries.

Equipment:

Gait parameters were recorded using the Cartesian Optoelectronic Dynamic Anthropometer (Codamotion) analysis system (Charnwood Dynamics Ltd., Leicestershire, UK). The Codamotion system is a widely used tool that has proven to be accurate and reliable in gait analysis research in capturing three-dimensional kinematics. The Codamotion system captures infrared light signals emitted by active markers that are attached to the body. Three CX1 CODA Sensor Units (receivers) were set up unilaterally to enable a 10 m 'capture' section of a 14 m walkway (Fig. 2a). Each participant wore six active markers—two on the right side of both feet (Fig. 2c), and two on the upper right upper limb/shoulder (one on the right side and one on the left).

Procedure:

The participants were broken up into four groups of four subjects, such that the same experiment was run four times on four separate occasions, with four participants in each experiment. There were only 24 markers available to run this equipment, which enabled a pod of four persons at a time. Allocation into each group was random or based on participant availability. On arrival at the motion capture laboratory, each participant provided informed consent as per the ethical approval granted by UCD. The length of upper arm, leg, shoe was recorded for each participant along with shoulder and hip width, height and weight. Six markers were attached to each person, one on the acromion process of the shoulder

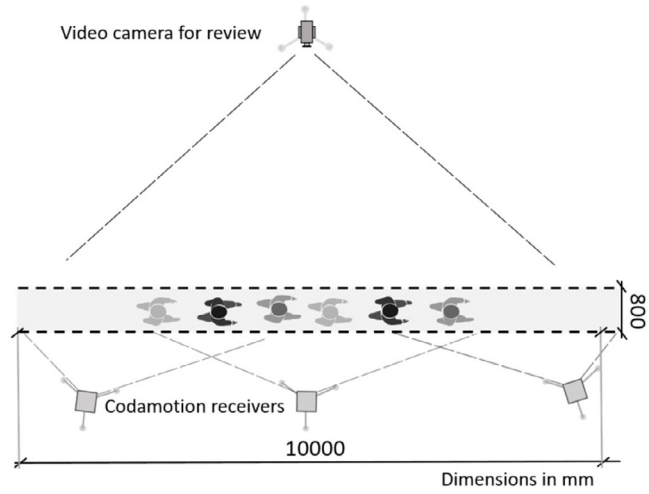


Fig. 2a. Schematic plan view of captured area.

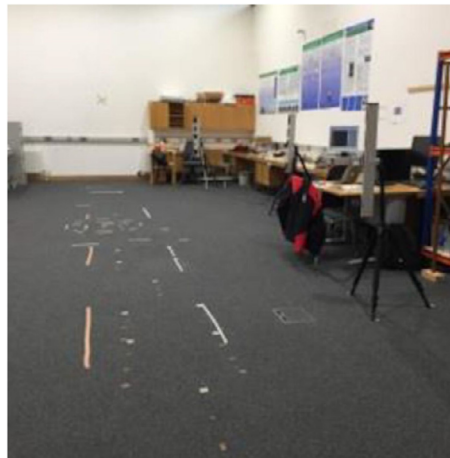


Fig. 2b. Photo of walkway at UCD.



Fig. 2c. Codamotion markers on feet.

Table 1
Experiment scenarios-number of participants and densities achieved.

| Trial (repeats) | No of participants | Density (Persons/m) |
|-----------------|--------------------|---------------------|
| A (3) | 59 | 2.87 |
| B (2) | 49 | 2.38 |
| C (2) | 39 | 1.90 |
| D (2) | 29 | 1.41 |
| E (4) | 24 | 1.17 |
| F (1) | 19 | 0.92 |

and half-way down the upper arm; and two on the right side of each foot, i.e., the side that faced the cameras, at the lateral aspect of the 5th metatarsal head and the posterior inferior lateral aspect of the heel for the right foot, and the lateral aspect of the 1st metatarsal head and posterior inferior medial aspect of the heel for the left foot. Heel markers were placed 3cms from the rear of shoe, accounted for in post-processing. These positions were chosen to optimise the visibility of the markers during walking and because these positions have previously yielded reliable stepping parameters.

The participants were asked to walk at specific speeds, in single file. Five specific speeds were chosen based on a review of the literature for very slow (0.2 m/s), slow (0.5 m/s), normal (1.0 m/s), fast (1.3 m/s) and very fast (1.7 m/s) walking speeds. The order of the speeds was randomised. The speed was controlled by one researcher walking in front who had practised pacing each speed, demonstrating excellent reliability, and who also listened to a metronome through earphones. The four research participants walked in single file with the instruction to follow the leader at a comfortable distance. Another researcher walked behind the four research participants so that each research participant was walking in the same condition, i.e., one person in front and behind them. Two trials at each speed were carried out, resulting in ten walking trials for each group of 4 participants on a 14 m straight line walkway. The sequence of the data capture with CodaMotion was recorded at 100 Hz within the 10 m capture area (Fig. 2a).

Data Processing:

Using the Codamotion software, a stick figure model was set up using the marker set worn by each participant to capture the data. The data was then exported to Excel. Inter-person distance was calculated using the distance between the shoulder marker of one person and the shoulder marker of the person in front. The positions of the extremity of the shoes were derived from the markers on the feet, from which contact buffer and step extent were calculated, as outlined below.

2.2. Experiment B (Lund University)

Experiment B describes tests carried out at the Lund laboratory, with larger numbers of subjects, analysed by using enhanced video analysis techniques, with virtual planes of measurement.

Participants:

Fifty-nine participants (aged 17–29 yrs, 22F; 37M) were recruited via a recruitment poster at Lund University, Sweden. Participants were rewarded with a cinema ticket each, for taking part, and were excluded if they were carrying any acute lower limb injuries.

Equipment:

The circuit comprised a 0.8 m wide path with a perimeter, measured at the centre line of 20.6 m, Fig. 3. Chairs were used to define the curved parts of the path, with the straight part of the path being defined by ropes (at the front, shown in red in Fig. 3a)) and a room partition (at the back). Three cameras (Sony HDR-PJ780/Sony HDR-CX220) were used in HD resolution to capture movement: one on the inside of the circuit, one on the outside of the circuit and one placed above the straight section. The use of ropes and partitions in the 4 m straight parts of the route, i.e. the measurement area, created physical barriers whilst maximising visibility of the key measurement points for the cameras.

Participants were identified in the experiments by unique numbers which were tagged to their right arm. Adhesive white stickers were used as markers to pinpoint specific points of interest, i.e. shoulder, hip, knee, tip of toe and heel, to facilitate the tracking for video analysis, Fig. 4b.

Procedure

On arrival at the test venue, participants went through a process of informed consent as recommended in the internal ethical review and risk analysis. Measurements were recorded of each participant's height, shoe length, ankle height, thigh length and shank length, Fig. 4. Participants were then assigned to different trials, each of which were designed to generate six different densities. The number of participants and generated densities are summarised in Table 1. Participants were instructed to walk in single file as they would naturally do given the number of people around them, i.e. without overtaking. The numbers of individuals, and hence the density, varied among the trials and the participants' walking speed varied accordingly.

Data Processing:

A software package, *Farrascope*, was custom-developed (by IAScience Ltd) to assist in the analysis of the videos in this experiment. *Farrascope* uses perspective reduction techniques and radial lens adjustment to remove measurement losses

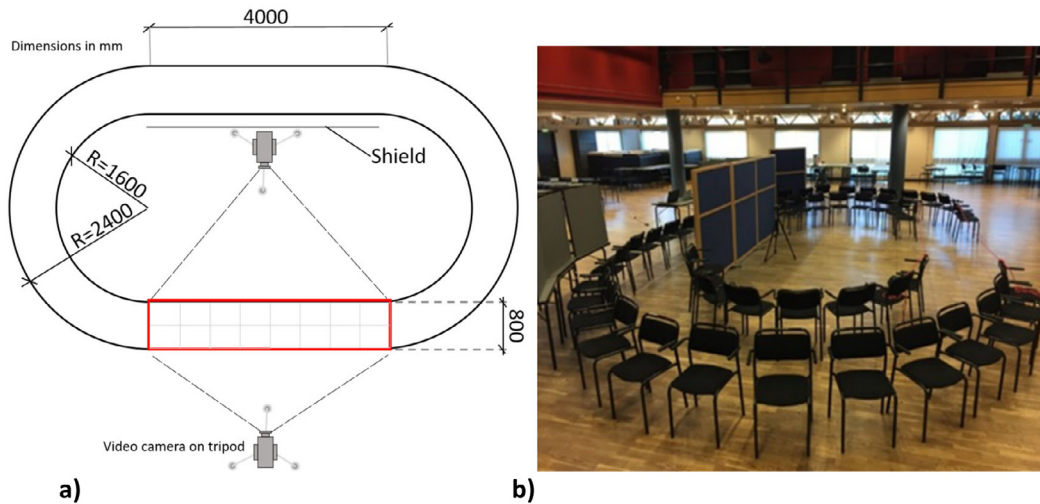


Fig. 3. (a) Schematic of the circuit (dimensions in mm) showing measurement area (red) and camera positions. (b) photograph of circuit.

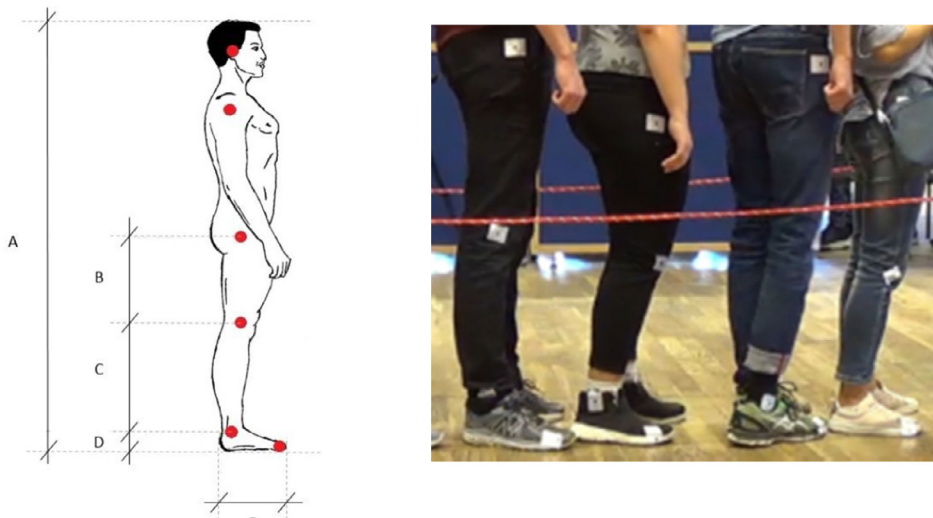


Fig. 4. (a) location of the tags attached to each participant and the dimensions measured: A (height), B (thigh length), C (shank length), D (ankle height), E (foot length). (b) markers to facilitate video analysis.

from the distance and lens distortion of the camera and hence facilitate more accurate quantification of the movement of identified points in the field of view of the fixed cameras.

The cameras were set up in position prior to the participants assembling for the tests. The videos recorded by the camera placed outside the circuit were used to calibrate Farrascope, track participants, and extract data points in these trials.

A 4.0 m × 1.0 m (in 0.5 m squares) grid was marked on the floor and test poles of 2 m height placed 3 m apart along the floor grid markings were used to provide reference scaling points for scaling and verification of the measurement system, Fig. 5. The measurement software has adjustments for radial distortion of the camera, in addition to supporting multiple planes of measurement in the depth of the field of view. The analyses used up to five planes of measurement: central along the marked pathway, 10 cm either side of the central line, to attempt to align with the planes of the left and right feet movements, and the front and back of the 4 × 1 m rectangle marked on the floor with 16 0.5 m × 0.5 m squares. This basic grid on the floor was used to provide multiple reference points for the planes of measurement in order to calibrate and verify the measurement processes. These grid lines were removed before starting trials. Prior to the analysis of the videos, verification tests were undertaken to check the accuracy of identified screen coordinate values against known real world measurements. Many points of reference were tested (mid-pole, floor etc.) and the accuracy was found to be ±1 cm with each pixel being less than 1 cm.

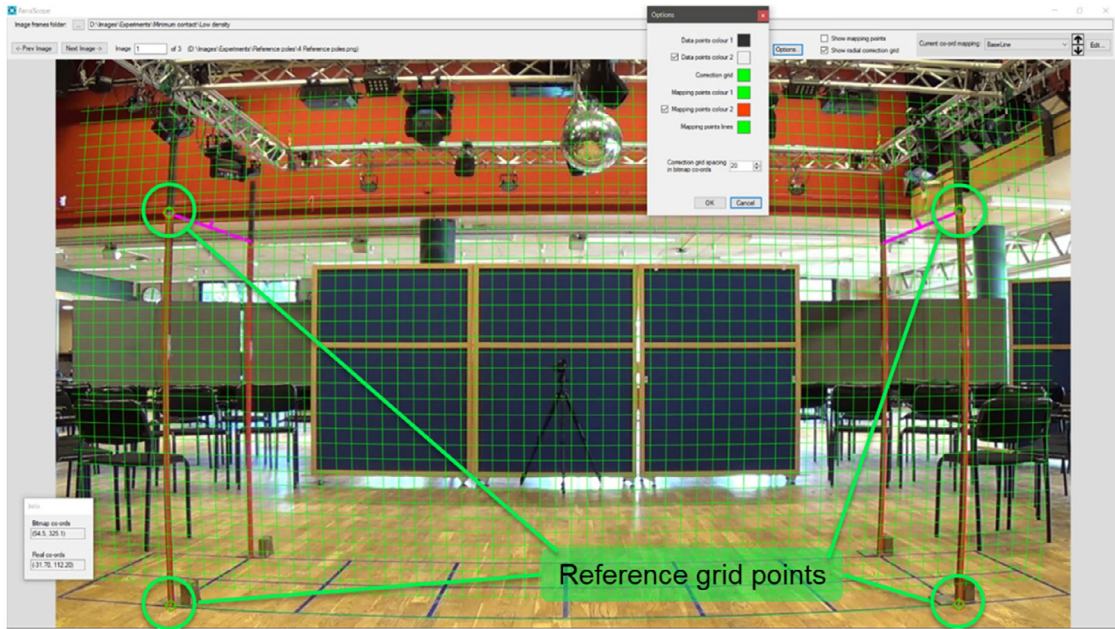


Fig. 5. Location of poles and reference grid points for planar measurement.

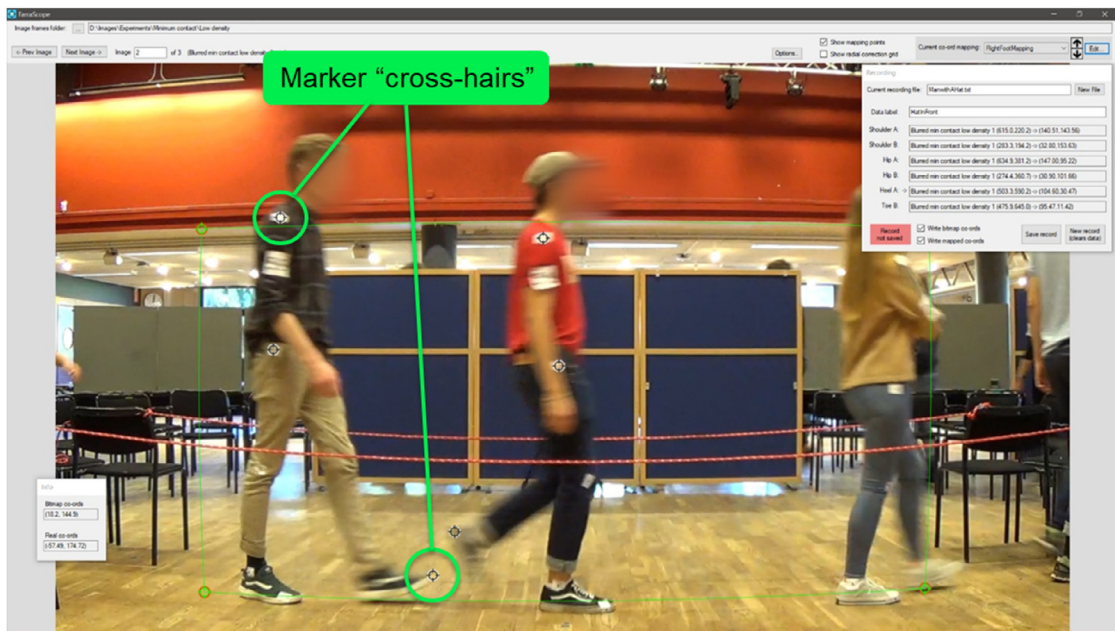


Fig. 6. Screen image of Farrascope highlighting “cross-hairs” tracking pedestrian markers.

The analysis followed the walking cycle of each participant within the area of interest, i.e., the 4 m straight part of the route. Each participant was tracked, one at a time, on a frame by frame approach to identify the heel strikes, point of minimum contact distance between them and the person in front and positions of hip and shoulder. A visualisation of the user interface of Farrascope showing markers being tracked is shown in Fig. 6.

It should be noted that, on occasions, markers became momentarily obstructed by an individual’s own or another person’s body parts. For example, a hip marker could be obstructed by an individual’s own arm or a foot marker may be obstructed by another individual’s foot. On those occasions, the positioning of the marker was estimated by considering the trajectory of the location of the marker immediately prior to, and immediately after, the time during which it was

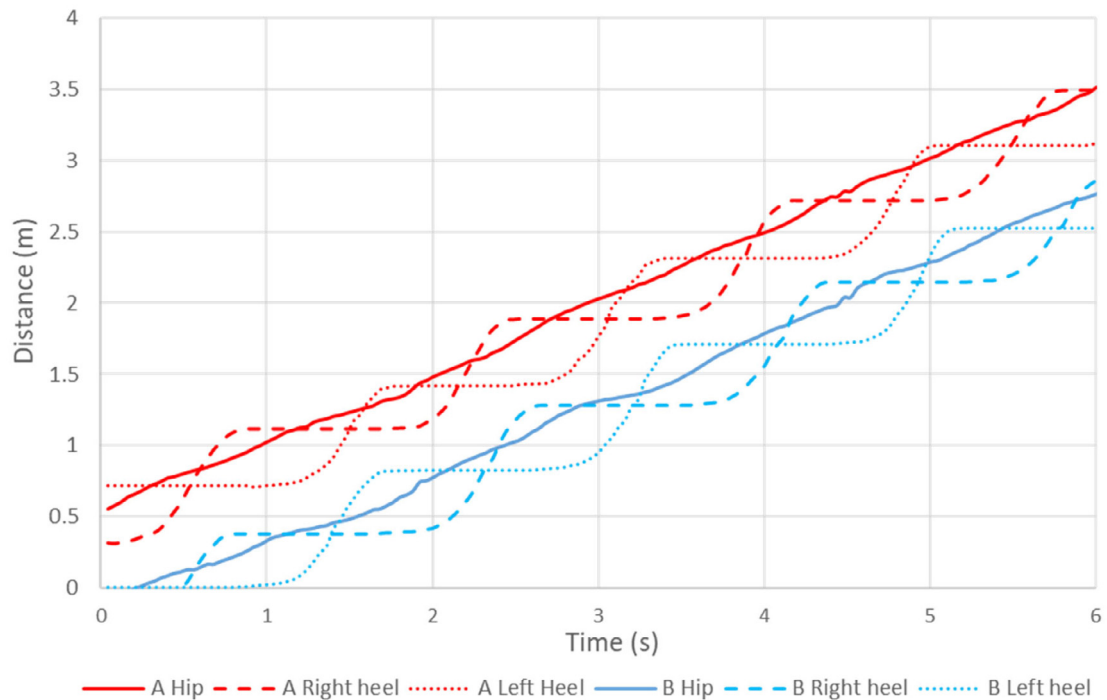


Fig. 7. Sample gait cycles, tracking heels of individuals A (ahead) and B (behind).

obstructed. The 3D dimensions for joint rotation, and changes in depth of field of view were not evaluated, in order to minimise analytical complexity. For this study, the 2D tracking position values (x as longitudinal ‘distance’, y as ‘elevation’) were measured to evaluate the model parameters, i.e., step length, step extent, inter-person distance and contact distance.

Some sample traces were also carried out for every frame to visualise the full tracked stepping cycle and interaction between individuals. For illustrative purposes, Fig. 7 shows typical synchronous gait cycles for participant B (behind) and participant A (in front). Asynchronous gait cycles would be similar, albeit out of phase.

The step length, maximum step extent (heel to toe) and minimum contact distance (toe to heel) for each step cycle was logged, and walking speed measured over the step cycle. The inter-person distance was also measured as the distance between the hip marker of the follower and the leader. Each participant was tracked individually, so the demographics could be cross-referenced against those recorded for each person at the outset. The number of recorded points, as expected, varied between the trials since participants in high-density trials tended to take shorter, and therefore more, steps within the measurement area compared to those in the low-density trials. This, however, meant an over-representation of data points in the higher density (lower walking speed) trials with approximately one third of the data points being representative of walking speeds below 0.2 m/s.

2.3. Calculations

In general, step lengths and step extents were normalised by the proportional adjustment of step for height or leg length, in the same standard way as other studies [16,18], for comparison purposes and to enable the results to be used later for populations with different heights or leg lengths. In Experiment A—UCD, data were normalised to the average height of 1.72 m (i.e. step lengths were multiplied by 1.72/participants height). In Experiment B—LUND, subjects were significantly taller (1.82 m) and in order to reduce further variability, we measured each participant’s individual leg length, so that we were able to normalise to the group mean leg length of 0.96 m instead. The implementation of more precise normalisation in the Lund data reflects a “learning” outcome of data processing from the UCD experiment. The Lund data could also, then, be further processed to normalise to the common height of 1.72 m that were used by most other studies including [21], and [16].

In both UCD and Lund experiments, the step length was measured as the distance between consecutive left/right heel strikes. The walking speed was calculated by dividing the distance travelled by the marker on the body by the step duration, with the shoulder marker being used at UCD and the hip at Lund. The speeds were, therefore, instantaneous speeds measured in each step. The step frequency was calculated as the inverse of the measured step duration in seconds for Lund, and by walking speed/step length for the UCD experiments, due to the slightly different methodologies of data collection. As a consequence of sampling at the step-cycle level, the charts of speed and step length may be more variable

than group-trends of other studies, but they do enable us to study more microscopic effects, in relation to the movement of each individual.

Gait analysis and crowd flow experiments commonly demonstrate a wide scatter of data above and below mean trend lines, and can also be subject to sampling bias where a standard fit curve would be affected by higher or lower sampling over one particular range. Other researchers such as [23] and [7] tackled this by taking aggregate bands of inter-person distance ranges, but banding by inter-person distance could prevent the charting of faster walking speeds, above the average preferred speed as slower and higher speeds in the same distance band become averaged out. Therefore, we aggregated our results by bands of walking speed in order that we would develop trends which included the speeds of the naturally faster participants. In order to calculate statistically meaningful trends which may be used for modelling in later studies, we also systematically tested the following regression lines for charts: linear, log-normal, second-order polynomial and third-order polynomial and stopped when the R^2 value increased by less than 0.05 from one to the next. Any exceptions to that rule are described and explained in the descriptive text accompanying each figure. For most charts, we have also shown the basic data plots (without banding) in order to clearly illustrate the inherent variability of the sampled data.

3. Results

The results are laid out in four subsections:

- 3.1 **the dynamic “gait cycle”** of two pedestrians (to inform the quantification of the “movement” and “contact/adaption” spatial components).
- 3.2 **the “step length and step extent”** quantifying the space taken up by the walking process: measured as the maximum step extent for each gait cycle (which is a function of the step length and foot length at an instantaneous point in the step cycle)
- 3.3 **the “contact distance”** quantified between points of potential foot contact, with the minimum value identified as the “contact buffer” representing the space left in between people for comfort and potential adaption to the movement of others in front.
- 3.4 **inter-person distance and the sum of the spatial components**— to see how the movement and adaption components may compare with the measured inter-person distances.

When reviewing the results in these subsections we have the core aims:

- develop an understanding of the basic dynamics,
- quantify both the physical space spanned by walking, and the “adaptive” space (“buffer”) between potential points of contact,
- evaluate these components against the inter-person distances.
- develop an understanding of how effective the different forms of measurement were, and also what would then comprise an effective strategy for future, related studies.

3.1. Dynamic “gait cycle” of two pedestrians in close proximity

Fig. 8 illustrates one sample “tracking” process of the gait cycle of two participants “A” (representing the person ahead) and “B” (the person behind) in the higher-density trials at Lund University. For clarity, it only shows the hip-marker and heel/ toe traces of the participants that were used to calculate the heel/toe contact and inter-person distances. Looking at the two solid-line hip traces, we can see that person A was about half a metre into the area of measurement at time ‘zero’ with person B walking behind and entering about quarter of a second afterwards. This trace was chosen specifically because it illustrates not only the dynamic nature of the interactions (during the step cycle) but also the magnitude of these variations at relatively close proximities.

In the higher-density trials, when participants were in very close proximity at lower speeds (~ 0.5 m/s) it became apparent that participants would adjust their gait very slightly sideways such that their heels and toes would overlap at the furthest extent of the step, and this was also the case if they were at standstill. This was evident, for example, at 2.7 s, in Fig. 8, when the toe trace of person B is further along the study area (1.6 m) than the heel of person A at about 1.4 m. In this case, it is the right-toe of B which is ahead of the left heel of A, but we also sometimes observed the heels and toes on the same side overlapping, with person B moving very slightly to one side to enable the step-cycle overlaps. These “overlaps” ultimately created negative contact distance values at the extent of the step cycle, which ultimately manifested themselves as slightly negative contact buffers in our charts.

Fig. 9 shows traces of the primary parameters under consideration at Lund, illustrating the variation of the heel-toe contact distance, the corresponding variations in step extent and the oscillations of inter-person distance (IPD) over time. Note that the step extent shown is the average of Person A and Person B, in order to relate to the distance in between the two individuals. This trace was chosen to demonstrate specific facets of the measurement process:

- the contact distance and step extent are approximately synchronised over each step cycle: the maximum step extent occurs at or just after the minimum contact distance (0 to 0.2 s after).

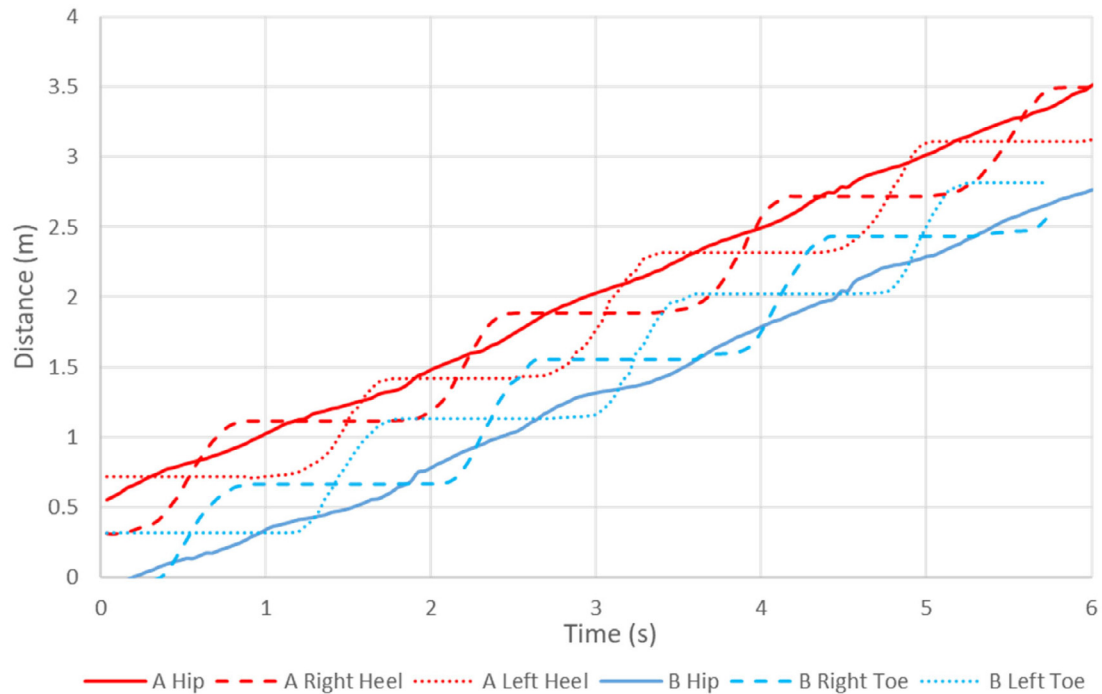


Fig. 8. Tracking heels of person A (ahead) and toes for person B (behind) – Experiment B – Lund.

- the inter-person distance oscillates above and below the mean (mean 72 cm \pm 7 cm) usually peaking about a quarter of a second before the step extent for each gait cycle.
- occasionally measurement errors are shown as small spikes (eg. at 1 s for the step extent) but this may sometimes be due to the manual process of aligning a marker with the end of the foot which could be blurred from the motion.
- the minimum contact distance for each step cycle (the ‘contact buffer’) varies by a similar magnitude to the measured inter-person distance. When ‘contact buffer’ is referred to across a spread of people and speeds, it usually represents the average contact buffer, and the value can be slightly negative when gait-cycles partly overlap.

3.2. Step frequency

The frequency of steps taken for the participants across the two experiments is shown in Fig. 10, in relation to tracked walking speed, with the trend being made more visible by using aggregated bands of 0.05 m/s (Fig. 10c). The step frequency has a higher variation at slower speeds than at higher speeds which reflects the more erratic nature of walking or ‘shuffling’ in very congested situations. Fig. 10c also suggests that in the lower speed range (up to 0–0.4 m/s) participants in the UCD experiments had a lower step frequency, for a given speed, than participants in the Lund experiments; this is consistent with the results presented in Fig. 11c (where participants in the UCD experiments had a longer step length for a given speed (Section 3.3)). The choices made by participants as to how to ‘achieve’ a given speed may reflect the different conditions of the two experiments i.e. in Lund the lower speeds were as a result of increased density and participants had more ‘pressure’ from behind, whilst in the UCD experiments the participants were walking in small numbers and following a leader at the given speed. The magnitudes of the reduced walking speed and reduced step frequency observed in the UCD tests were similar to those observed by [28] in single-person “free walking” experiments, where the range measured was 0.5 m/s to 2.0 m/s, which may further indicate the different nature of the two tests.

Because there were fewer people in the field of view, and less group pressure to move forward, the UCD subjects waited for people in front to move further ahead before then taking a longer/faster step. Given that the speed measured was the instantaneous speed in one step cycle, there were occasions where the step speeds were higher than the average speed. It should be noted that a few outlying values of 3.5 steps/second were regarded as sampling errors and were removed from the data sets.

3.3. Step length and step extent

The usual measure for length of space occupied by locomotive movement in the gait cycle for single file flow is step length, which is measured between points of successive left/right heel strikes on the ground. It was important to

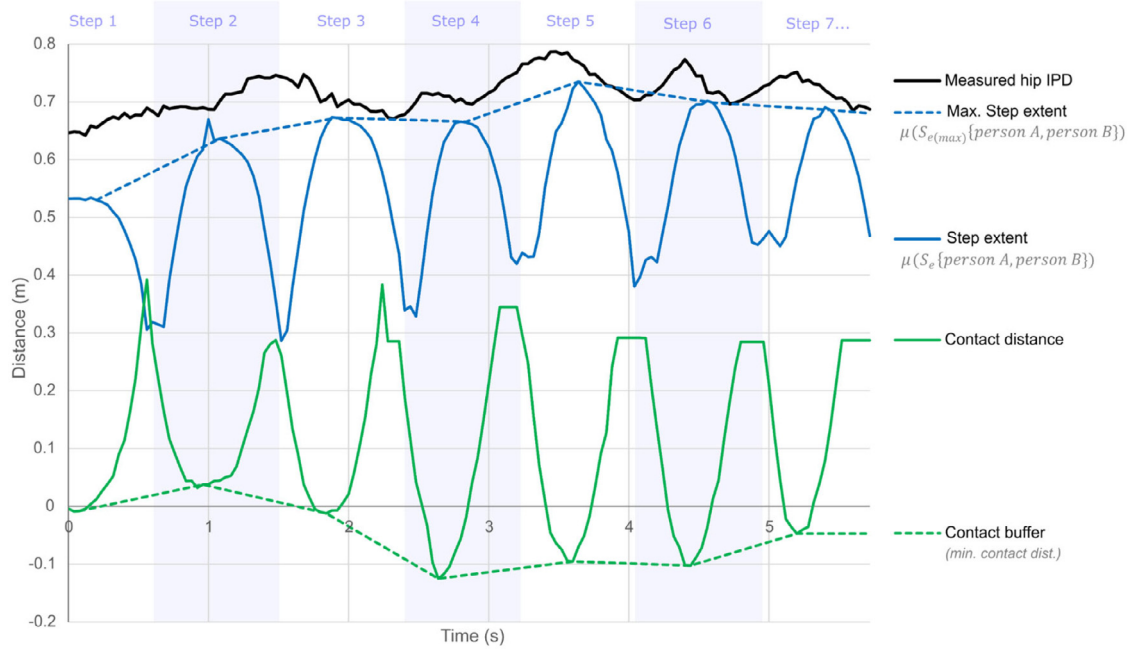


Fig. 9. Tracking contact distance & step extent with gait cycles over time.

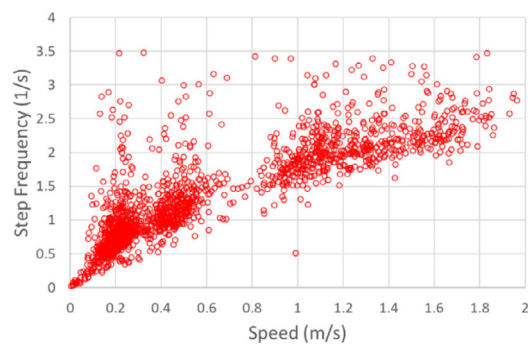


Fig. 10a. UCD step frequency vs speed data.

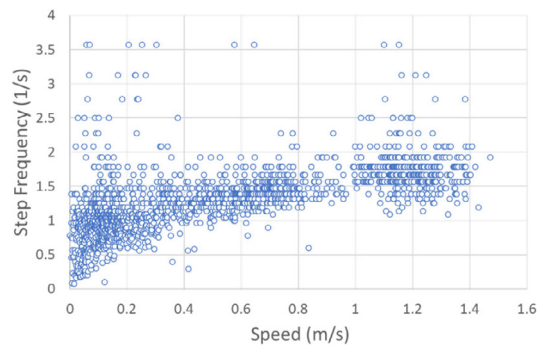


Fig. 10b. Lund step frequency vs speed data.

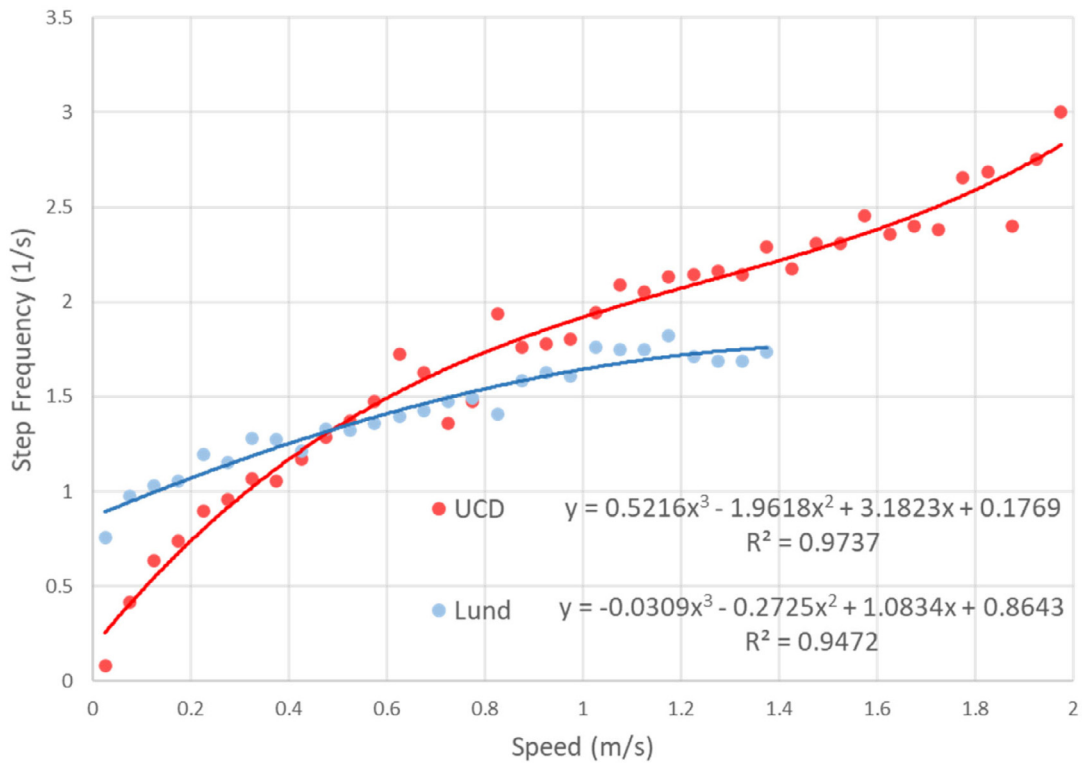


Fig. 10c. Step frequency vs speed with data points aggregated in bands of 0.05 m/s.

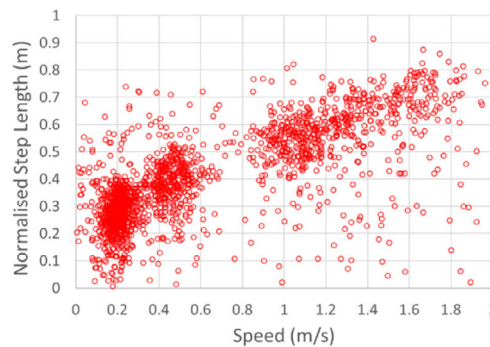


Fig. 11a. UCD step length vs speed data.

measure the step length in both experiments to compare with each other and with previous studies. It is evident from the measurements of step length in Figs. 11a and 11b that we oversampled at lower speeds (because we sampled every step cycle, and there are more step cycles at lower speeds). Aggregated speed bands were therefore used to compensate for sampling bias in the results.

Figs. 11a and 11b show that the data points plotted for the UCD experiment have a wider spread of values than for Lund because the few participants were generally further apart, and less ‘pressured’ to keep a close distance. Visual inspection of the videos suggested that there was less synchronisation of individual gait cycles in the Lund experiments, compared to UCD, and this may be explored more quantitatively in future analyses. An actual increase in the point values for step length below 0.175 m/s was further evidence of the more erratic and less “pressured” walking behaviour in the UCD experiment, particularly at low speeds. For the UCD step length data we observed an actual increase in step length at low speeds (less than 0.2 m/s). This at first seems unintuitive, but if we consider the step frequency at these low speeds for the UCD data, Fig. 10a, we can see that it was extremely low at these speeds and it was observed that there was a much greater tendency for “stop and go”—essentially, that people would wait for nearly 25 cm space before stepping ahead. Participants under these relaxed, non-constricted conditions often waited until they had a significant amount of space

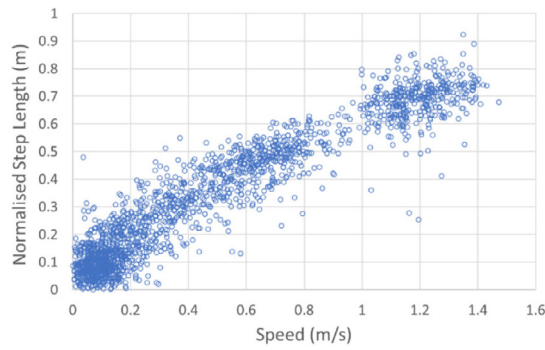


Fig. 11b. Lund step length vs speed data.

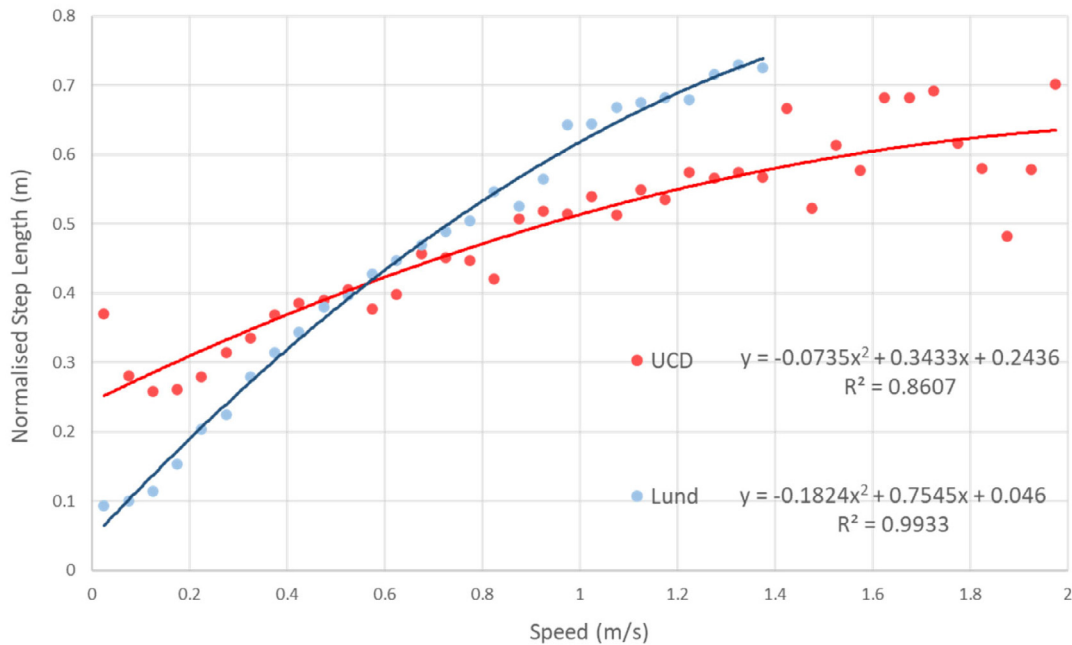


Fig. 11c. Step length vs speed (with normalised data, aggregated in 0.05 m/s speed bands).

to move into until they made any move forward, leading to a greater reduction of step frequency and lower reduction of step length, when compared to Lund. In contrast, at higher speeds, we observed slightly shorter step lengths as they approached the end of the measurement area.

For the Lund data, the trends in the step length were more in line with expectations; the base curve polynomial fit trends to only 4.6 cm for step length at zero speed, showing that people shuffled forwards by a few centimetres when space was available and also possibly shuffling their feet forwards and back occasionally.

It should also be noted that some experimental error is inevitable with video analysis at these low speeds because it is not always possible to see the exact end of the toe and heel as step cycles overlap.

Comparison of the relationships between step length and walking speed established in this study with other studies, Fig. 12, suggests that the Lund curve (with the step length normalised to a (common average normalisation) height of 1.72 m aligns closely with that of [29], [15] and [21].

While step length is measured over the duration of one step cycle, it is related to the instantaneous value of maximum “step extent”. Fig. 1 showed a typical mid-density situation where the max. step extent would be similar to, but up to 10% less than the sum of the step extent and the foot length (from our observations). In addition, from Eq. (2), the “step extent” should (in theory) be exactly equal to foot length when the participants are standing still at zero speed.

Fig. 13 shows the step extent at different speeds for Lund and UCD experiments with best fit 2nd order polynomials. Note that we did consider a 3rd order polynomial fit for these charts, but this did not provide any significant benefit in R^2 value.

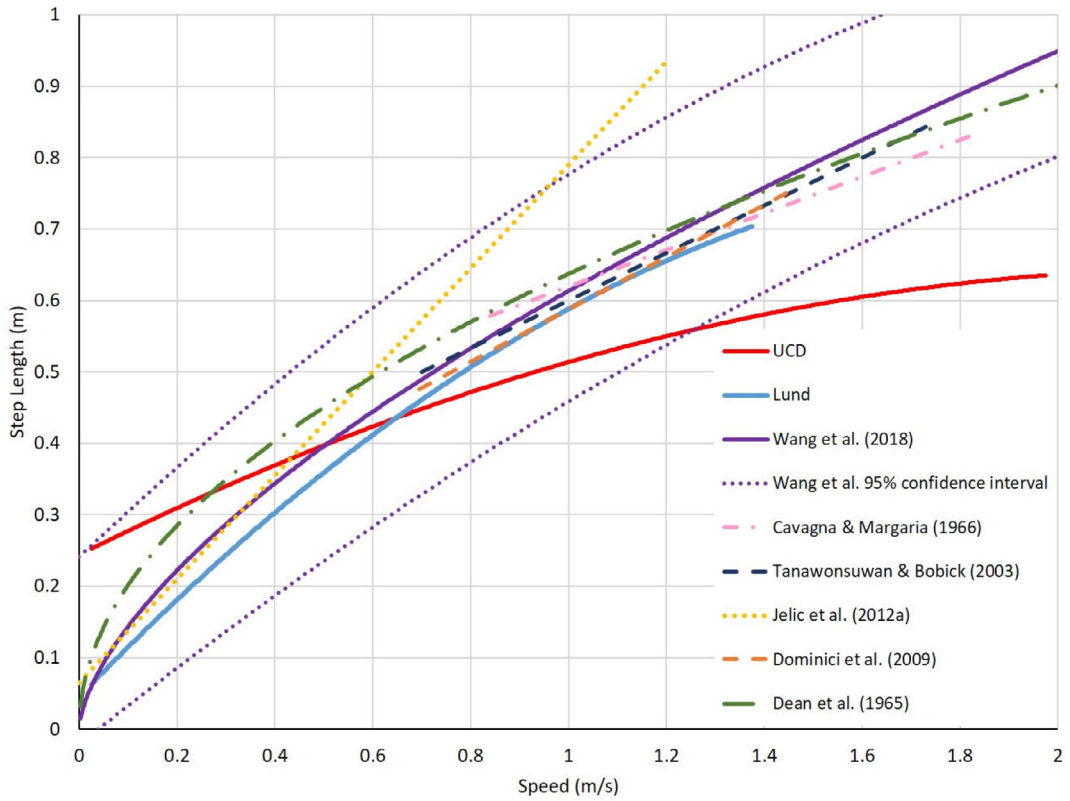


Fig. 12. Step length vs speed trends in different studies (normalised to 1.72 m height).

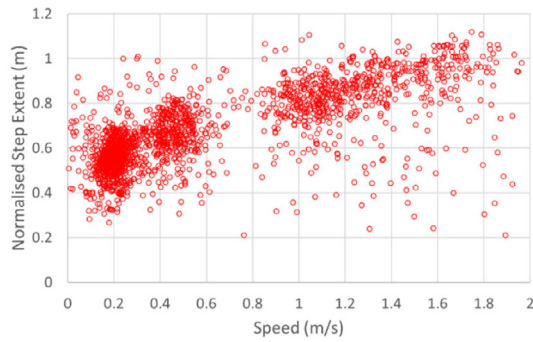


Fig. 13a. UCD step extent vs speed data.

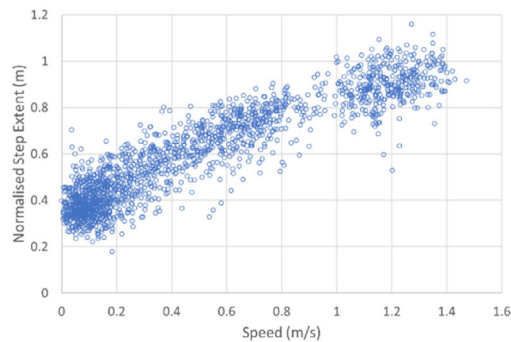


Fig. 13b. Lund step extent vs speed data.

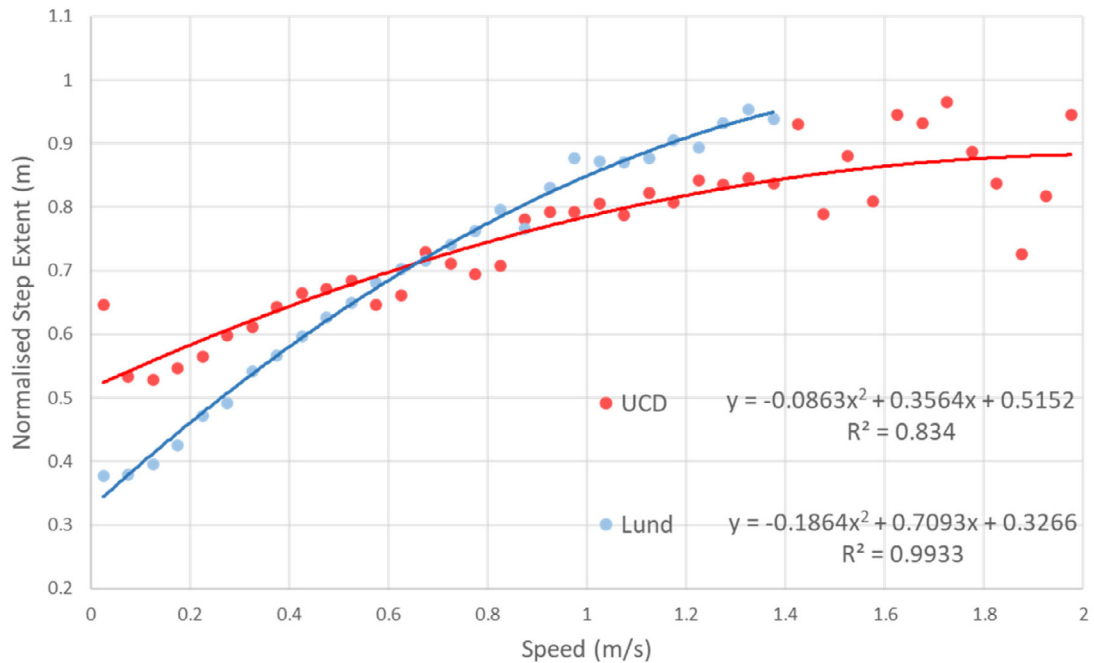


Fig. 13c. Step extent vs speed (with normalised data, aggregated in 0.05 m/s speed bands).

Fig. 13c indicates that, at higher speeds, the UCD participants' steps were shorter than the Lund participants' steps at higher speeds; this is consistent with the shorter step lengths illustrated in Fig. 11c. There also appears to be a wider spread of banded data at the higher speeds, but that could be at least partially caused by the lower sampling frequency at the higher speeds. Fig. 10c shows how much the step frequency increased in the UCD experiments in order to compensate for the flattening off of the step length at higher speeds. As Fig. 11 illustrates, the Lund data stopped at the naturally comfortable speed of the participants, where no additional high speed trials were carried out, and enforced higher speeds would have been challenging to achieve in the experimental setup. Additionally, it is useful to note that the polynomial fitted intercept of step extent at zero speed is 0.327 m for the Lund tests, which is only 0.04 m greater than the average shoe length, indicating that the movement for these tests showing that participants moved to a "short shuffle" when they started moving, whereas UCD participants moved only when they had a larger space ahead.

The relationship between step extent, step length and foot length

Step extent is always expected to be less than the sum of the step length and foot length because it represents the maximum extent of the step cycle at any given point in time, rather than the total extent of the step cycle measured between the times of consecutive heel/floor strikes. From Eq. (2), we can consider the step extent as a proportion of step length and foot length, and essentially that the ratio, i.e., factor "A" in Eq. (2) is equal to the step extent/(step length+foot length). This factor is of particular interest because it potentially enables us to consider the step length (which we know is related to demographics such as height and age) as the basis to potentially derive the maximum step extent, and potentially predict the "movement space" for different cohorts in future work.

The variation in this ratio (factor A) is illustrated in Fig. 14, and fit curves are applied in order that we can define mathematical derivations for the terms in Eq. (2), potentially relating to demographics. This enables maximum step extent to be derived from step lengths (which have been measured and approximated for different cohorts). These data can then potentially be used for predictive models of crowd movement in future work

3.4. Contact distance and contact buffer

The "contact buffer" shown in Fig. 1 is measured as the minimum contact distance between heel and toe in these single file flow tests, Eq. (1). It is postulated that this is the space that the pedestrian leaves to be able to cope with sudden changes in movement of the person ahead, and to adapt his or her own movement in order to avoid a collision contact; simply put, they maintain a distance such that they will not walk into the person in front. The contact distance will vary over the time of each step cycle, as shown previously in Fig. 9.

The contact buffer values (the minimum contact distance measured for each step cycle) are plotted in Fig. 15. It is evident that there is considerable scatter in both experiments reflecting the variable nature of different individuals and step cycles. We had initially expected a lower scatter of data for the UCD experiment because of the relatively high

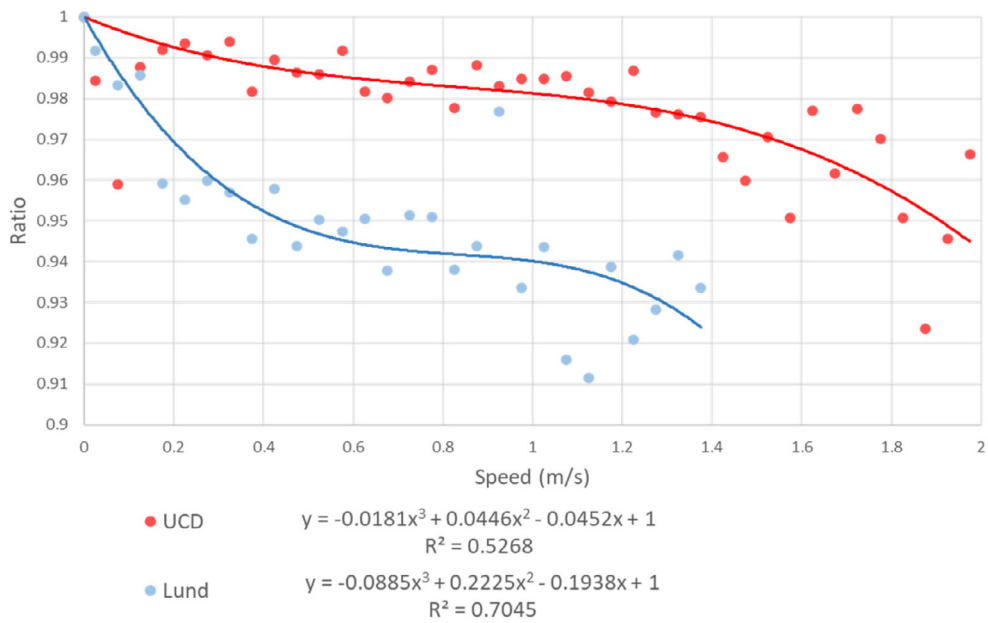


Fig. 14. Step extent as a proportion of step length + foot length in speed bands.

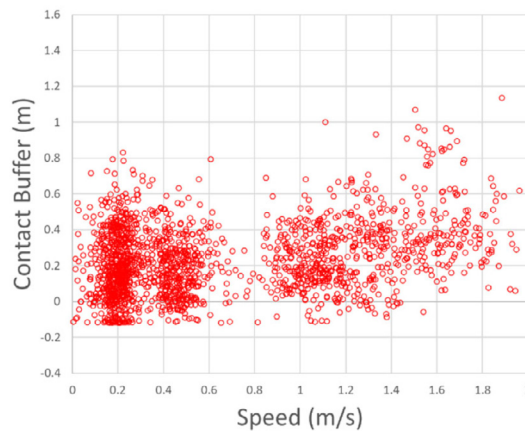


Fig. 15a. UCD contact buffer vs speed data.

accuracy of the motion-capture apparatus, but instead we observed a significantly higher scatter of data, which generally seemed to be due to the more erratic, less constrained nature of the movement in the UCD experiments compared to Lund.

The trends for contact buffer become clearer when the data is banded by speed. In general, there is a “flattening off” of the contact buffer towards the minimum value of natural, queued spacing at standstill. Multiple forms of regression fit were tested: linear, power, 2nd-order and 3rd order polynomials, but the best fit (highest R^2 value) was achieved by using a two-line fit, with minimum value, and linear gradient, similar to the form tested in initial prototype work (Thompson et al. 2020). The first set of points used for the constant minimum were chosen where the collective mean value yielded an even number of points above and below the line, with a simple linear regression fitted for the points afterwards. It should be noted that the rising linear regression gradient (distance/speed) converts (by units) to a time, which may be considered to be the time that a person leaves to allow them to adapt to the dynamic environment. This adaptive time (gradient) for rising walking speeds was 0.184 s for UCD data at speeds above 0.694 m/s, and 0.381 s for Lund data above 0.386 m/s, as people transitioned from low-frequency shuffling to more regular walking. The UCD gradient was potentially lowered by the final, lower value at 1.95 m/s, where only 6 points were aggregated.

It can be observed that higher contact buffers were observed in the UCD experiment compared to Lund for speeds below approx 1.1 m/s. Once again the likely reasons for this are the low number of participants in the UCD experiment

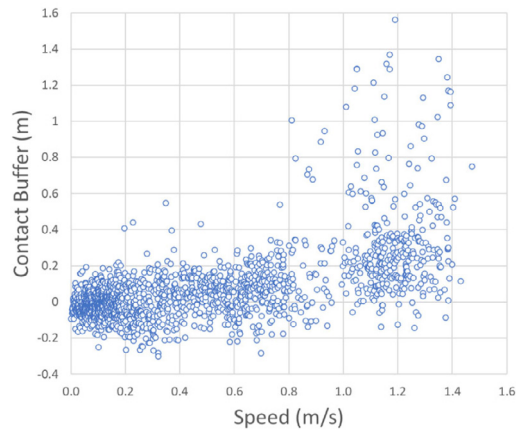


Fig. 15b. Lund contact buffer vs speed data.

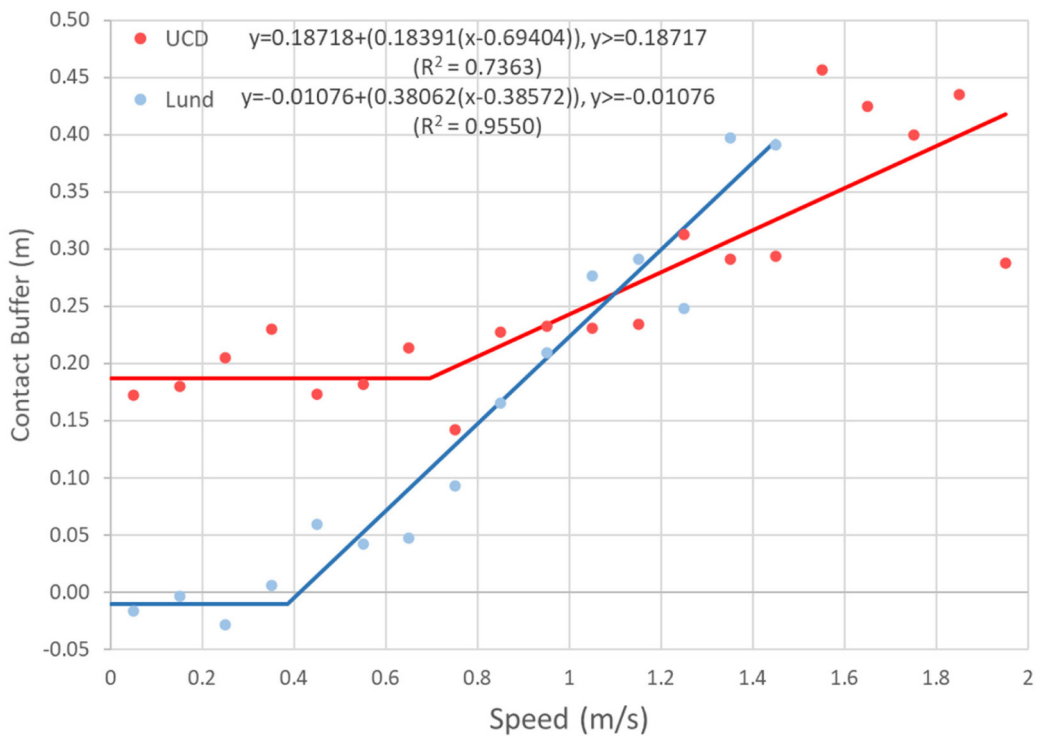


Fig. 15c. Contact buffer vs speed (with data aggregated in 0.05 m/s speed bands).

and the less pressured nature of the experimental protocols; in UCD participants were free to choose when to move at their own speed behind the leader, but Lund participants were subject to different density conditions and ‘pressured’ by other individuals. It is also evident that in the Lund experiments at speeds below 0.4 m/s, the contact buffer is negative, representing an overlap between the steps of the leaders and followers.

3.5. Inter-person distance and the sum of the spatial components

Inter-person distance (IPD) vs speed. The inter-person distances were measured between hip markers of Person A to Person B for the Lund experiments and between the shoulder markers for the UCD experiments. These values were sampled at the same time as the maximum step extent for each step cycle, and are illustrated in Fig. 16.

The positive linear relationship between inter-person distance and speed yielded a reasonable statistical fit in the Lund experiments. The “stop and go” movements in the UCD tests may have contributed to a lower value of R^2 in the

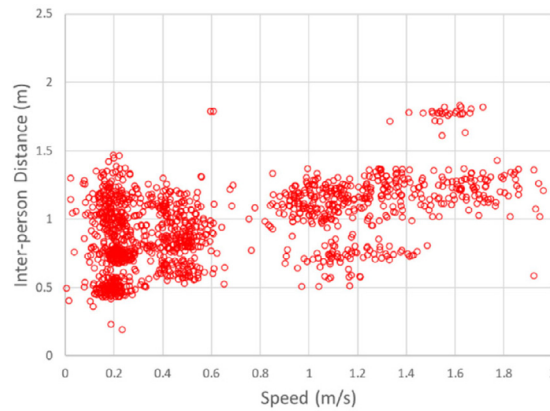


Fig. 16a. UCD IPD vs speed data.

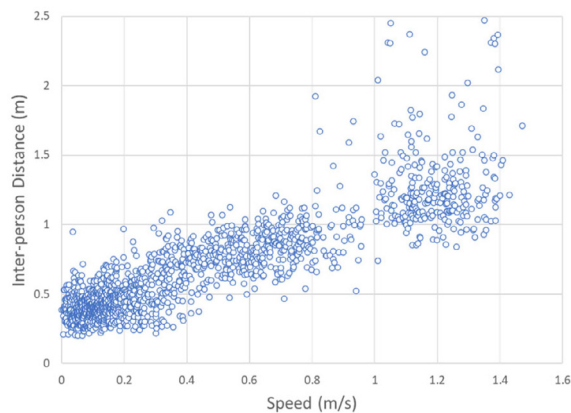


Fig. 16b. Lund IPD vs speed data.

statistical fit for a linear regression here. A comparison of the relationship established in this study to that of others (for inter-person distances < 1.1 m) is illustrated in Fig. 17. It should be noted that other researchers measured inter-person distance in different ways, for example Cao et al. measured head-to-head distance of participants, and banded by inter-person distance.

It is evident that there is a much greater IPD for UCD participants at lower speeds, again due to the fact that we had a smaller sample of participants (only 4) in the area of study, and there was less “pressure” to move forwards and ample space to keep comfortable distances; often participants waited for comfortable space ahead before starting to move, creating the aforementioned “stop and go” patterns. Encouragingly, the Lund results seem to fit quite well within the spread of other experimental studies.

Table 2 lists the gradient and intercept (at zero speed) of the linear fit for IPD vs speed in different studies.

The gradient, as interpreted before by [22,23] and [7], is expressed with the units of time and named “adaption time” by [17]. This value can show the sensitivity of the person behind to the distance from the person in front. The gradients for the Swedish (Lund) experiments and the French [17] experiments are very close (within 0.02 s).

The intercept represents the minimum inter-person distance at standstill conditions. The intercept value for the Lund single file experiment is very similar to the results of the experiment conducted by [22] and close to the results of experiments conducted by [17]. This value (0.35 m) is greater than the studies conducted by [24] and [7] that have very close IPD gradient values (0.22s and 0.25s respectively). This could be a result of the differences in body size, height (body dimensions of Europeans tend to be slightly larger than statistically averaged Chinese and Indian body dimensions [30] and cultural norms. It should also be mentioned that participants in [24] study were only males. Interestingly, for the Chinese and Indian tests, if we subtract the foot length from IPD at standstill (intercept) we see negative distance values which may indicate overlapping steps at high densities.

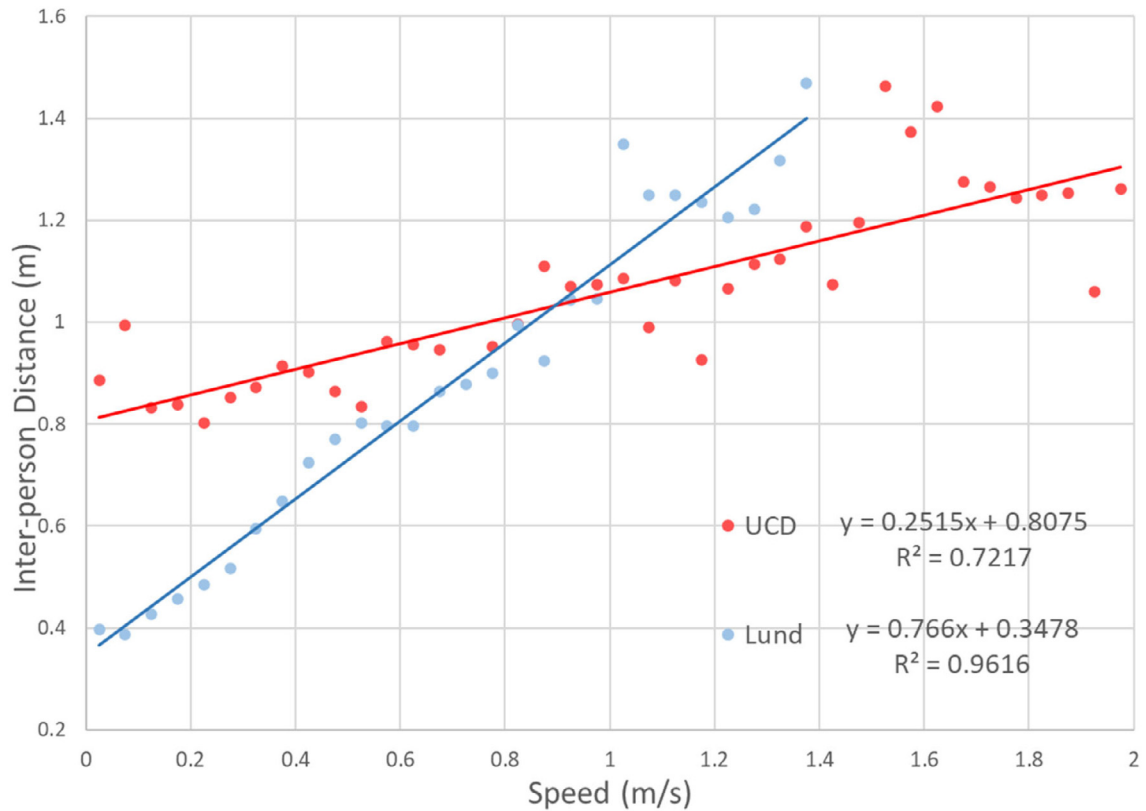


Fig. 16c. Inter-person distance vs speed (with data aggregated in 0.05 m/s speed bands).

Table 2

Lists the gradient and intercept(at zero speed) of the linear fit for IPD vs speed in different studies.

| Reference (Country) | Cohort | IPD/speed (gradient, s) | IPD at standstill (intercept, m) |
|---------------------------|---------------------------------------|-------------------------|----------------------------------|
| UCD, this paper (Ireland) | Students | 0.25 | 0.81 |
| Lund, this paper (Sweden) | Students | 0.77 | 0.35 |
| [7] (China) | Young students | 0.69 | 0.25 |
| | Young + elderly mix | 1.31 | 0.25 |
| [23] (France) | Male + female mix, young adult | 0.75 | 0.45 |
| [22] (Germany) | Students and staff | 1.06 | 0.36 |
| [24] (India) | Male grad. students & technical staff | 0.89 | 0.22 |

3.5.1. Comparing inter-person distance with the sum of the “step extent and contact buffer”

Fig. 18 illustrates the tracking of the inter-person distance (using the hip markers) of the same two sample participants shown in Fig. 9 in the Lund experiments whilst in the measurement area. The trace shows the degree of experimental variation that can occur for the same two people in the same sample over time. This chart also shows the contact buffer + step extent (average of max. for Persons A and B) to illustrate how the time-based addition of the “sum of the components” matches the inter-person distance (Eq. (4)). While the inter-person distance varies by about 0.15 m during the period, and the sum of the step extent and contact distance varies by 0.25 m, these cycles of variation are not exactly synchronised. A good example of the synchronisation of the two plotted values is shown during the first full step cycle between 0.5 and 1.4 s, two traces overlap closely during the centre of the step cycle. The step cycles tracked afterwards show a wider variation, due to variations in stance and gait cycle.

Figs. 19a and 19b illustrate the testing of Eq. (3), by showing the sum of the contact buffers and maximum step extents for the step cycles, plotted with the measured inter-person distances (sampled across all our tests, at the same times for Lund data and UCD respectively).

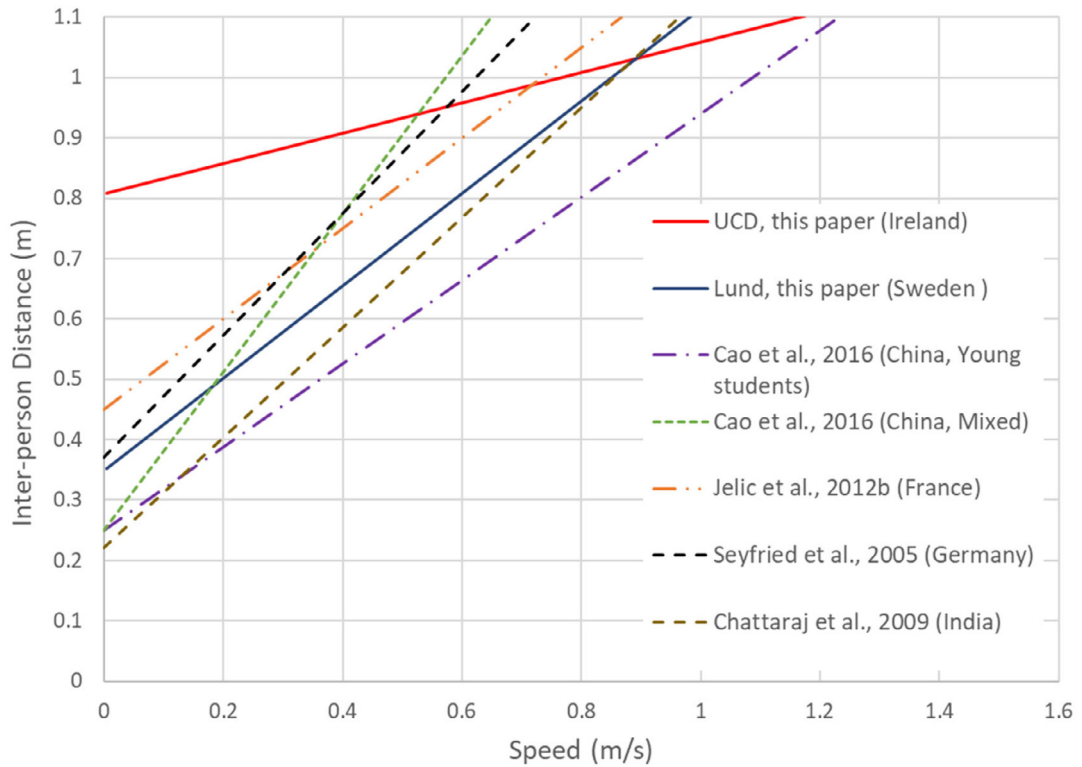


Fig. 17. Inter-person distance (IPD) vs speed trends in different studies.

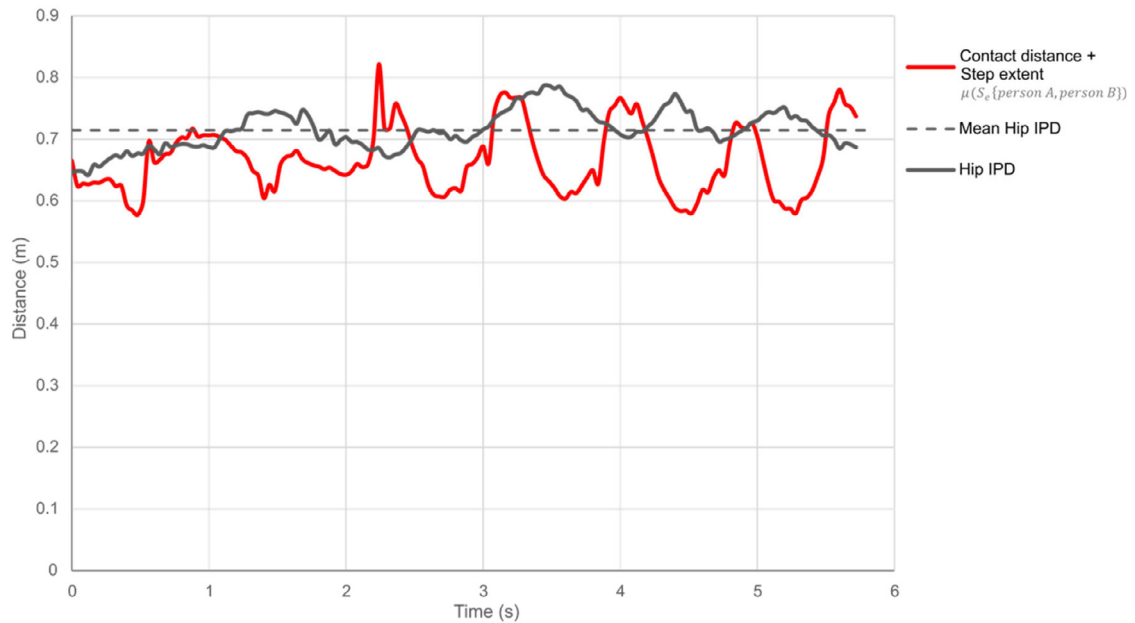


Fig. 18. Tracking Inter-person distance (IPD) and the sum of C_d and S_e over time.

Fig. 19a shows an encouraging alignment between the sum of the components (“maximum step extent + contact buffer”) and the measured IPD (± 5 cm) at speeds below 0.3 m/s and above 1.15 m/s in the Lund experiments. Some wider variations were observed in the mid-range of speeds.

Fig. 19b shows a wider disparity between the measured inter-person distance and the sum of the spatial components (nearly 30 cm), which may be a consequence of the erratic nature of the “stop and go” behaviour of the participants in their less congested surroundings.

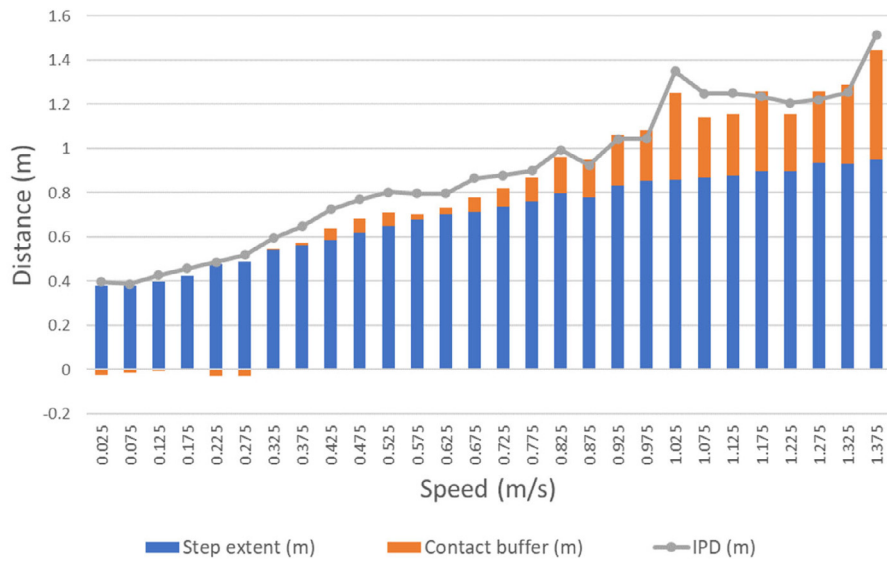


Fig. 19a. Comparing inter-person distance with spatial components for Lund data.

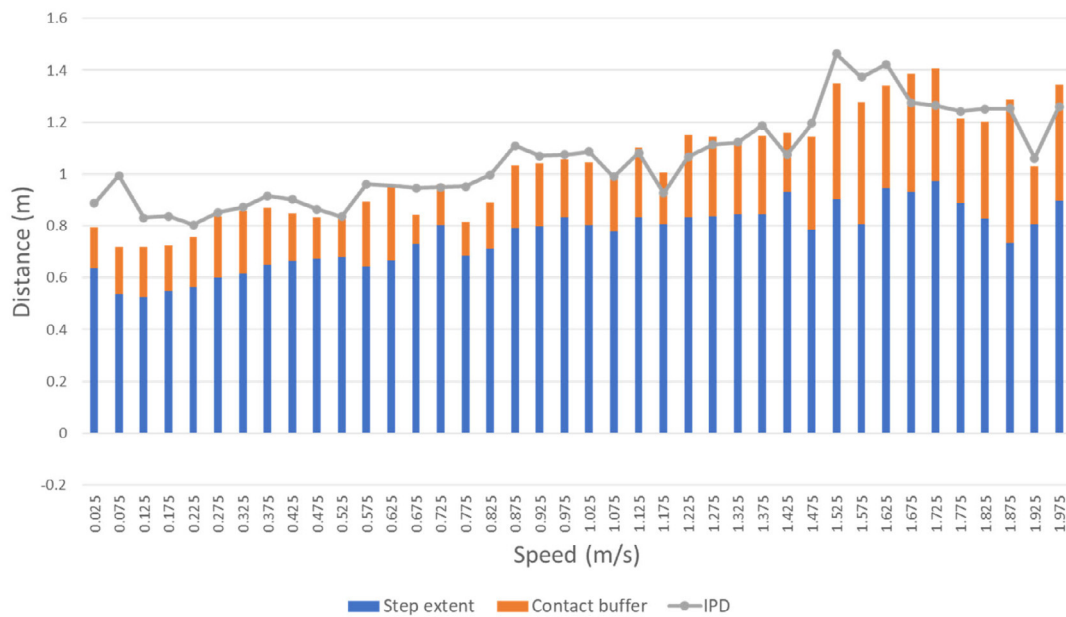


Fig. 19b. Comparing inter-person distance with spatial components for UCD data.

The average of the distances between the banded values across the trials show the “sum of the components” to be 4.3 cm and 3.1 cm lower than the measured IPD for the Lund data (video capture) and UCD data (motion capture) respectively. These results are encouraging, especially given that we know that there will be some experimental errors causing a few centimetres variation, described in the Lund test methods.

4. Discussion

Reviewing the outcomes of measuring the step extent and contact buffer

Other studies into crowd movement have generally analysed a selection of the inter-person distance, crowd flow, crowd speed or step length, but this paper highlights the importance of quantifying the two separate components of stepping movement and contact space together. To be able to measure these components and find that they sum, on average, to a

value within a few centimetres of the inter-person distance may be regarded as a successful outcome, especially given the experimental limitations. It is also encouraging that the Lund results seemed to recreate the step length trends observed by other researchers, while further quantifying the components of step extent and contact buffer.

The UCD experiments did not reflect congested conditions because of the small number of test subjects and the controlled walking speeds, but rather reflected a situation akin to a situation in which individuals have a bound velocity due to a slower leader but still have some freedom to choose the distance from their leader. Although the inter-person distances could be small, the same psychological pressure on occupants in a crowd to move forward did not exist in these sparsely populated scenarios. They were, however, successful in showing that the experimental equipment enabled the measurement of the contact buffer and step extent. Additionally, while the magnitude of the contact buffer and step extents varied significantly from the Lund tests, they did show forms of similar statistical trends. Budget and equipment availability were the main reasons why these markers were not fitted for large scale tests.

The Lund tests showed good alignment with similar tests, for step length changes with walking speed in congested space. It is anticipated that the form of the step extent and contact buffer charts, developed from these tests may form the basis of work for wider applications. The equations for the fit curves were included for every chart in order that these components could be implemented in future computer models. If future mathematical or computer models are based on step extent and contact buffer, then these two components may be related to age and demographics, which would allow the field to begin deriving crowd movement from the base demographics of the populations. For example, the step extent formulae are based on normalised values, which could be re-normalised to a different person's height. The preferred walking speeds are known for different cohorts (young, elderly, children, mixed ability etc. described by [31]) and it may also be possible to adapt the curve fit in Fig. 15 to a minimum contact-distance with rising linear fit. The linear relationship of speed and distance converts to time, and it might then be possible to relate that contact-spacing to cognitive and biomechanical response time.

Experimental limitations, accuracy, and further development

Between the two sets of experiments, we did achieve the desired outcome: demonstrating the successful use of new or adapted techniques to measure more detailed components of pedestrian dynamics than previously quantified. However, we considered data accuracy issues and limitations which are described below.

In the UCD experiments, using optical motion sensors:

- were more quantitatively accurate than the video analysis experiments with each point being approx. ± 0.2 mm (dividing receiver resolution by the capture area length); these automatically collected data points were not prone to any manual error that may be associated with the marker identification process in the video analysis adopted in the Lund experiments.
- used the marker at the acromion process (shoulder) to calculate inter-person distance, as this marker was in view almost all of the time. There may have been as much as ± 2 cm variation through oscillations in stance and torso rotation at specific times. However, this was both positive and negative around the data set, which should, to some extent, be statistically counteracted by the adoption of the aggregated data bands in the charts.
- encountered very occasional occlusion artefacts, which were compensated by the data capture software using spline interpolation to estimate the missing points. This only happened on rare occasions, and is not considered to be of computational significance.
- only allowed for 4 participants to be tracked at any time due to constraints on the number of markers available. Practicalities aside, more participants could potentially be measured in a larger capture volume, but their scope would remain within single-file flow analyses.

In the Lund experiments, using video capture and analysis:

- the optical accuracy of measurement was ± 1 cm for the video processing to quantify visually clear body or foot edges, with one screen pixel-width usually representing less than 1 cm.
- despite extensive training with the same researcher, on-screen manual clicking of the markers may have introduced some errors. For example, the heel and toe measurements were manually identified at the tip of the toe and the back of the heel, rather than the marker, for better accuracy to use directly in the model. This may have caused errors in calculating the step length and step extent. The feet were often moving quite quickly and were sometimes blurred, so manual judgement calls needed to be made when locating feet-end extents. These errors may be in the range of approximately $\pm 1-2$ cm.
- additional possible errors may be observed with the coordinate system, defined in 2 dimensions, i.e. in the middle of the path through the walking direction (x) and the height (y). Therefore, there was no depth axis, but instead different discrete measurement planes, at different distances from the camera. Participants' legs rarely aligned perfectly with these ideal measurement planes, but having multiple planes of measurement (for left foot, right foot/shoulder) at least attempted to compensate for the variable field of depth. We did do multiple measurement cross checks with known points of measurement on camera, and the measurements were within $\pm 1-2$ cm centimetres.

The Lund video processing could be further improved by:

- using higher quality video cameras, with a higher resolution (eg. 4 k), faster frame rate and shutter speed to remove motion blur. It would also be interesting to investigate the effects of changing camera positions to reduce radial distortion effects.
- using small high-visibility circular markers at the very ends of the shoes which might be easily and (more importantly) automatically tracked on camera to make more of the data collection more automatic and less open to human error or bias.

In previous studies, inter-person distances have been measured from different points i.e. head to head (often termed headway), hip to hip or shoulder to shoulder. In Experiment B (Lund University), for higher densities, upper body rotation was observed when participants occasionally communicated or viewed the circular path ahead (verified by separate pilot eye-tracking recordings undertaken as part of this experiment, unpublished). No significant differences were observed when comparing average inter-person distances using the shoulder or hip markers in this experiment – variations in upper and lower body segments expected to cancel each other out. We decided to use the hip marker for better accuracy in examining steps individually. Given that the shoulder marker was used to determine inter-person distance in Experiment A (UCD), we recognise that absolute comparisons between experiments would pose a problem, and we did not seek to do this statistically. The use of both aggregated bands and applying a best fit curve for both studies are intended to compensate for that.

Additional studies for wider flow were carried out at Lund, with cameras on both sides, and these are being further developed. The system can be expanded to wider flows, potentially up to two lanes, using two cameras synchronised with overhead cameras to measure multi-lane flow. In those scenarios, the torso, shoulder and arm distances may need to be considered as potential points of contact, so will be expected to be more complex. Quantifying the additional components and lane formations in wider flow are a clear, natural, future development of these investigations.

5. Conclusions

These two novel experiments have successfully quantified the parameters of pedestrian movement identified as step extent, contact distance (varying during the gait cycle), and contact buffer (minimum contact distance) in addition to their relationship with the established variables of walking speed, step length and inter-person distance.

The step length, step extent and contact buffer all increased with increased walking speeds, as people transitioned from shuffling to more natural gait movement, in less congested conditions. The quantification of the parameters and their inter-relationships showed that the:

- *step length* and *step frequency* both increased to achieve greater walking speeds (Figs. 10c and 11c).
- *step extent* decreased from 100% to 92% of step length as walking speed increased to 1.3 m/s (the mean unimpeded walking speed) (Fig. 14) in the single loop tests at Lund. The reduction in step extent was less pronounced in the single-line tests (at UCD) for all speeds, likely due to the less congested surrounding conditions within the experiments.
- *contact buffer* was observed to be a negative and constant value at low speeds and high density, due to overlapping steps (Fig. 8) and “shuffling” behaviour in the Lund tests.
- an ‘*adaption time*’ of 0.38 s was derived from the linear gradient of contact buffer versus walking speed as people transitioned to slightly higher walking speeds, in reduced congestion in the measured section of the loop at Lund. This confirms that adaption time should therefore be part of the future development of the mathematical model.
- *inter-person distance* closely aligns to the sum of the maximum step extent and the contact buffer (within the variance of experimental error and the gait cycle oscillations) which shows encouraging agreement with the proposed mathematical model.

The basic mathematical model can incorporate best fit equations for the parametric relationships (Figs. 11c, 14, 13c, 15c, 16c), which has positive implications for future modelling. Step length is related to the demographics of height, leg length, age and walking ability, and these factors will therefore be used to inform the model. In addition, it is anticipated that adaption time will be related to age and cognitive abilities, as it is in traffic flow. Therefore, these factors may be incorporated into the model such that inter-person distances, crowd speed, and crowd flow may potentially be estimated for different population demographics. While the mathematical model can potentially incorporate demographics, further experimental work is required to quantify the values in relation to these differing demographics parameters. Future developments of the model and parameters will be aligned with updates to experiments and processes, for validation and verification purposes.

CRedit authorship contribution statement

Peter Thompson: Conceptualization, Methodology, Software, Validation, Formal analysis, Investigation, Data curation, Writing – original draft, Writing – review & editing, Visualization, Supervision. **Hossein Tavana:** Methodology, Software, Validation, Formal analysis, Investigation, Data curation, Writing – original draft, Writing – review & editing, Visualization. **Cathy Goulding:** Methodology, Software, Validation, Formal analysis, Investigation, Data curation, Visualization.

Supervision. **Håkan Frantzich**: Conceptualization, Methodology, Validation, Resources, Writing – original draft, Writing – review & editing, Visualization, Supervision, Project administration, Funding acquisition. **Karen Boyce**: Conceptualization, Methodology, Validation, Formal analysis, Investigation, Data curation, Writing – original draft, Writing – review & editing, Visualization, Supervision. **Daniel Nilsson**: Conceptualization, Methodology, Validation, Resources, Writing – original draft, Writing – review & editing, Visualization, Supervision, Project administration, Funding acquisition. **Gabriel Larsson**: Formal analysis, Investigation, Data curation. **Jesper Friholm**: Formal analysis, Investigation, Data curation. **Denise McGrath**: Conceptualization, Methodology, Validation, Data curation, Writing – original draft, Writing – review & editing, Visualization, Supervision.

Declaration of competing interest

The authors declare the following financial interests/personal relationships which may be considered as potential competing interests: Hakan Frantzich reports financial support was provided by Swedish Fire Research Board (Brandforsk). Hakan Frantzich reports financial support was provided by SFPE.

Acknowledgements

The authors would like to express their sincere gratitude to:
 – Bob Farrel of IAScience, for writing Farrascope specifically for this project, and which is now being used on other projects
 – Silvia Arias of Lund University for help and guidance with first-phase post-processing of results.

Funding

The experimental work and initial analysis was funded and supported by Brandforsk (the Swedish Fire Research Board) who kindly funded the experimental work, grant no. 200-161; Crowd safety: prototyping for the future. Showing how the science for “pedestrian flow” can keep up with demographic change [32].

The first-phase post-processing was funded by The Society of Fire Protection Engineers (SFPE), United States who funded first phase post processing as part of grant: “Determining evacuation capability with biomechanical data” [33]

These contributions and funding made this work possible and are highly appreciated.

References

- [1] B.D. Greenshields, J.R. Bibbins, W.S. Channing, H.H. Miller, A study of traffic capacity, in: Highway Research Board Proceedings, Vol. 1935, National Research Council (USA), Highway Research Board, 1935.
- [2] M. Shi, E.W.M. Lee, Y. Ma, W. Xie, R. Cao, The density-speed correlated mesoscopic model for the study of pedestrian flow, *Saf. Sci.* 133 (2021) 105019, <http://dx.doi.org/10.1016/j.ssci.2020.105019>.
- [3] K. Teknomo, Application of microscopic pedestrian simulation model, *Transp. Res. F Traffic Psychol. Behav.* 9 (1) (2006) 15–27, <http://dx.doi.org/10.1016/j.trf.2005.08.006>.
- [4] Department of Economic and Social Affairs (DESA), Population Division, 2015, World Population Ageing 2015, United Nations, New York, 2015.
- [5] OECD, Obesity update, organisation for economic cooperation and development, 2017, Available from: <https://www.oecd.org/els/health-systems/Obesity-Update-2017.pdf>. (Accessed 2 September 2017).
- [6] K. Boyce, Safe evacuation for all-fact or fantasy? Past experiences, current understanding and future challenges, *Fire Saf. J.* 91 (2017) 28–40, <http://dx.doi.org/10.1016/j.firesaf.2017.05.004>.
- [7] S. Cao, J. Zhang, D. Salden, J. Ma, R. Zhang, Pedestrian dynamics in single-file movement of crowd with different age compositions, *Phys. Rev. E* 94 (1) (2016) 012312, <http://dx.doi.org/10.1103/PhysRevE.94.012312>.
- [8] P. Thompson, D. Nilsson, K. Boyce, M. Molloy, D. McGrath, Exploring the biomechanics of walking and crowd flow, *Fire Mater.* 44 (6) (2020a) 879–893, <http://dx.doi.org/10.1002/fam.2889>.
- [9] J.J. Fruin, *Pedestrian Planning and Design*, Metropolitan Association of Urban Designers and Environmental Planners, 1971.
- [10] J.L. Pauls, Movement of people, in: P.J. DiNenno, C.L. Beyler, R.L.P. Custer, W.D. Walton, J.M. Watts Jr., D. Drysdale, J.R. Hall Jr. (Eds.), *The SFPE Handbook of Fire Protection Engineering*, National Fire Protection Association, Quincy, MA, 1996, 3–263–3–285.
- [11] J.L. Pauls, J.J. Fruin, J.M. Zupan, Minimum stair width for evacuation, overtaking movement and counterflow—technical bases and suggestions for the past, present and future, in: *Pedestrian and Evacuation Dynamics 2005*, Springer, Berlin, Heidelberg, 2007, pp. 57–69, http://dx.doi.org/10.1007/978-3-540-47064-9_5.
- [12] P. Thompson, D. Nilsson, K. Boyce, D. McGrath, Evacuation models are running out of time, *Fire Saf. J.* 78 (2015) 251–261, <http://dx.doi.org/10.1016/j.firesaf.2015.09.004>.
- [13] C. Kirtley, M.W. Whittle, R.J. Jefferson, Influence of walking speed on gait parameters, *J. Biomed. Eng.* 7 (4) (1985) 282–288, [http://dx.doi.org/10.1016/0141-5425\(85\)90055-X](http://dx.doi.org/10.1016/0141-5425(85)90055-X), In this issue.
- [14] M.J. Seitz, G. Köster, Natural discretization of pedestrian movement in continuous space, *Phys. Rev. E* 86 (4) (2012) 046108, <http://dx.doi.org/10.1103/PhysRevE.86.046108>.
- [15] R. Tanawongsuwan, A. Bobick, Performance analysis of time-distance gait parameters under different speeds, in: *International Conference on Audio-and Video-Based Biometric Person Authentication*, Springer, Berlin, Heidelberg, 2003, pp. 715–724, http://dx.doi.org/10.1007/3-540-44887-X_83.
- [16] G.A. Dean, An analysis of the energy expenditure in level and grade walking, *Ergonomics* 8 (1) (1965) 31–47, <http://dx.doi.org/10.1080/00140136508930772>.
- [17] A. Jelić, C. Appert-Rolland, S. Lemerrier, J. Pettré, Properties of pedestrians walking in line. II. Stepping behavior, *Phys. Rev. E* 86 (4) (2012a) 046111, <http://dx.doi.org/10.1103/PhysRevE.86.046111>.

- [18] J. Wang, M. Boltes, A. Seyfried, J. Zhang, V. Ziemer, W. Weng, Linking pedestrian flow characteristics with stepping locomotion, *Physica A* 500 (2018a) 106–120, <http://dx.doi.org/10.1016/j.physa.2018.02.021>.
- [19] D.W. Grieve, R.J. Gear, The relationships between length of stride, step frequency, time of swing and speed of walking for children and adults, *Ergonomics* 9 (5) (1966) 379–399, <http://dx.doi.org/10.1080/00140136608964399>.
- [20] Y. Morio, K.P. Izawa, Y. Omori, H. Katata, D. Ishiyama, S. Koyama, Y. Yamano, The relationship between walking speed and step length in older aged patients, *Diseases* 7 (1) (2019) 17, <http://dx.doi.org/10.3390/diseases7010017>.
- [21] J. Wang, W. Weng, M. Boltes, J. Zhang, A. Tordeux, V. Ziemer, Step styles of pedestrians at different densities, *J. Stat. Mech. Theory Exp.* 2018 (2) (2018b) 023406, <http://dx.doi.org/10.1088/1742-5468/aaac57>.
- [22] A. Seyfried, B. Steffen, W. Klingsch, M. Boltes, The fundamental diagram of pedestrian movement revisited, *J. Stat. Mech. Theory Exp.* 2005 (10) (2005) P10002, <http://dx.doi.org/10.1088/1742-5468/2005/10/P10002>.
- [23] A. Jelić, C. Appert-Rolland, S. Lemerrier, J. Pettré, Properties of pedestrians walking in line: Fundamental diagrams, *Phys. Rev. E* 85 (3) (2012b) 036111, <http://dx.doi.org/10.1103/PhysRevE.85.036111>.
- [24] U. Chattaraj, A. Seyfried, P. Chakroborty, Comparison of pedestrian fundamental diagram across cultures, *Adv. Complex Syst.* 12 (03) (2009) 393–405, <http://dx.doi.org/10.1142/S0219525909002209>.
- [25] G. Zeng, S. Cao, C. Liu, W. Song, Experimental and modeling study on relation of pedestrian step length and frequency under different headways, *Physica A* 500 (2018) 237–248, <http://dx.doi.org/10.1016/j.physa.2018.02.095>.
- [26] P. Thompson, *Developing New Techniques for Modelling Crowd Movement (Phd thesis)*, University of Edinburgh, 1994.
- [27] M. Boltes, A. Seyfried, Collecting pedestrian trajectories, *Neurocomputing* 100 (2013) 127–133, <http://dx.doi.org/10.1016/j.neucom.2012.01.036>.
- [28] M.D. Latt, H.B. Menz, V.S. Fung, et al., Walking speed, cadence and step length are selected to optimize the stability of head and pelvis accelerations, *Exp. Brain Res.* 184 (2008) 201–209, <http://dx.doi.org/10.1007/s00221-007-1094-x>.
- [29] N. Dominici, E. Daprati, D. Nico, G. Cappellini, Y.P. Ivanenko, F. Lacquaniti, Changes in the limb kinematics and walking-distance estimation after shank elongation: evidence for a locomotor body schema? *J. Neurophysiol.* 101 (3) (2009) 1419–1429, <http://dx.doi.org/10.1152/jn.91165.2008>.
- [30] S. Lee, R. Bro, Regional differences in world human body dimensions: the multi-way analysis approach, *Theor. Issues Ergon. Sci.* 9 (4) (2008) 325–345, <http://dx.doi.org/10.1080/14639220701511713>.
- [31] L. Ferrucci, R. Cooper, M. Shardell, E.M. Simonsick, J.A. Schrack, D. Kuh, Age-related change in mobility: perspectives from life course epidemiology and geroscience, *J. Gerontol. Ser. A Biomed. Sci. Med. Sci.* 71 (9) (2016) 1184–1194, <http://dx.doi.org/10.1093/gerona/glw043>.
- [32] D. Nilsson, P. Thompson, D. McGrath, H. Boyce, *Crowd safety: prototyping for the future: Summary report showing how the science for pedestrian flow can keep up with demographic change*, *Fire Saf. Eng.* (3231) (2020).
- [33] P. Thompson, H. Frantzich, S. Arias, J. Friholm, *Determining Evacuation Capability with Biomechanical Data*, Brandteknik, LTH. Report 7048., Lund University, Lund, 2020b, 2020. ISRN: LUTVDG/TVBB–7048–SE.